JOURNAL OF GEOMAGNETISM AND GEOELECTRICITY

VOL. VIII NO. 3

SOCIETY
OF
TERRESTRIAL MAGNETISM AND ELECTRICITY
OF
JAPAN

SEPTEMBER 1956
KYOTO

JOURNAL OF GEOMAGNETISM AND GEOELECTRICITY

EDITORIAL OFFICE: Society of Terrestrial Magnetism and Electricity of Japan, Geophysical Institute, Kyoto University, Kyoto, Japan

The fields of interest of this quarterly Journal are as follows:

Terrestrial Magnetism	Aurora and Night Airglow
Atmospheric Electricity	The Ozone Layer
The Ionosphere	Physical States of the Upper Atmosphere
Radio Wave Propagation	Solar Phenomena relating to the Above Subjects
Cosmic Rays	Electricity within the Earth

The text should be written in English, German or French. The price is set as 1 dollar per number. We hope to exchange this Journal with periodical publications of any kind in the field of natural science.

The Editors

Intensity Problem in the Deflection of Cosmic Rays in the Solar Magnetic Field

By Teiichiro YAGI

Physical Institute, Nagoya University

(Read May, 1951, Received Oct. 1, 1956)

Abstract

Assuming uniform parallel beam of cosmic rays at infinity is deflected in the general magnetic field of the sun, cosmic-ray intensities at each point of the earths' orbit were calculated. Problem was treated only in the equatorial plane for simplicity. As the intensities change with season, the solar diurnal variation averaged over all season never tends to zero due to the heliomagnetic deflection of cosmic rays.

We will assume that there exists a anisotropic distribution of cosmic rays in a space outside the solar system, due to any origin. This origin, for instance, may be the rotation of our galaxy, well known as Compton-Getting effect.[1] Because of the deflection of cosmic-ray particles by the sun's general magnetic field, apparent solar diurnal variation of cosmic rays will show an annual variation not only in its phase, but also its amplitude. Thus, even if this apparent solar diurnal variation will be averaged over one year, it will not vanish and remain as mean solar diurnal variation. In order to study this possibility, following calculation was carried out. Deflection of cosmic rays in the solar magnetic field was already calculated in our previous paper,[2] which will be denoted as [1] hereafter, and this work is continuation of [1].

Now, problem was treated only in the equatorial plane, under the assumption that the sun's and the earth's magnetic dipole moment are parallel to each other. In Fig. 1, M_s is the sun's dipole moment, which is directing towards the back of paper perpendicular to the plane of paper, that is, towards the negative direction of Z-axis. Circle C is the earth's orbit and P is the position of earth, which is designated by radius r_s and angle φ_s counted positively clockwise from Y-axis. Now, we assume that there exists a uniform parallel beam of cosmic rays parallel to Y-axis at infinity. Furthermore,

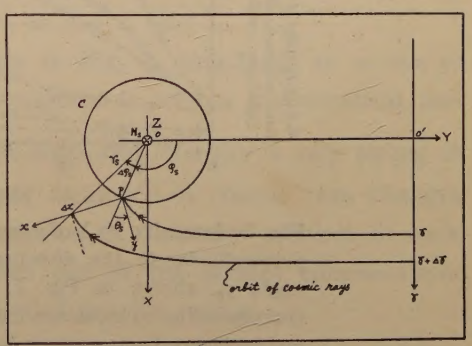

Fig. 1 Circle C is the earth's orbit and P is the position of earth. Axes and symbols used in the paper are shown.

we take γ-axis perpendicular to Y-axis at sufficiently far distance from the earth and x-axis perpendicular to the direction of incidence of cosmic rays at P, and we consider that particles existing in the region $\gamma \sim \gamma + \Delta\gamma$ at infinity are incident into the region $0 \sim \Delta x$ at P. Then, if we denote cosmic-ray intensities per unit time per unit area perpendicular to the direction of incidence of cosmic rays at infinity and at P as $j(\gamma)$ and $j(\varphi_s)$ respectively, then

$$j(\varphi_s)dt\,dx\,dZ = j(\gamma)dt\,d\gamma\,dZ.$$

If we take the direction of x-axis in a definite way and $j(\gamma) \equiv 1$, then

$$j(\varphi_s) = \left|\frac{d\gamma}{dx}\right| = \left|\frac{\partial\gamma}{\partial\varphi_s}\frac{d\varphi_s}{dx} + \frac{\partial\gamma}{\partial r_s}\frac{dr_s}{dx}\right| = \left|\frac{\cos\theta_s}{r_s}\frac{\partial\gamma}{\partial\varphi_s} + \sin\theta_s\frac{\partial\gamma}{\partial r_s}\right|, \tag{1}$$

where lengths are measured in Störmer's unit and γ is two times γ_1, which appears in [1].

$\frac{\partial\gamma}{\partial\varphi_s}$ and $\frac{\partial\gamma}{\partial r_s}$ were computed by differentiating the curve $\varphi_s(\gamma_1, r_s)$, which was obtained at the study of [1] and is shown in Fig. 4 a and 4 b of appendix 1. So, of course, the accuracy of computation is rather low. Intensities $j(\varphi_s)$ thus obtained is shown in Fig. 2, where full line and dotted line are two branches with different directions of incidence of cosmic rays as already mentioned in [1]. From this, it is

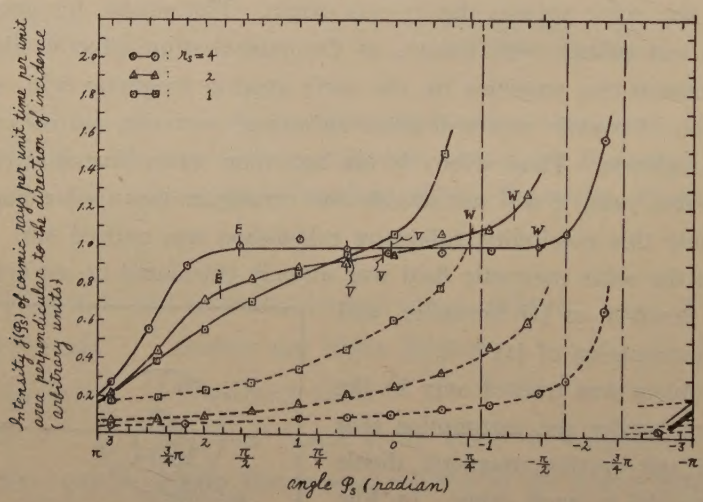

Fig. 2 Intensity $j(\varphi_s)$ of cosmic rays per unit time per unit area perpendicular to the direction of incidence are plotted against angle φ_s, shown in Fig. 1. Points, E, V, and W are those corresponding to incidence from eastern horizon, vertical incidence, and incidence from western horizon. The parts E-V-W of curves correspond to outer orbit.

recognized that intensity changes with season and there exists gloomy season covered with magnetic shadow and light season. Still more, twilight is incident after rotating many times around the sun, which is not shown in Fig. 2 wholly and extension of short line appearing at the right end of Fig. 2.

Here, we will see how the direction of incidence of cosmic rays changes on x-axis. In Fig. 3, angle of incidence θ_s is counted positively eastwards from PO′. (In the paper [1], θ_s was counted positively eastwards from PO′ for outer orbit and from PO for inner orbit, respectively.) About the angle α from x-axis to the direction of incidence of cosmic rays, it is easily seen that $\Delta\alpha=\Delta\theta_s-\Delta\varphi_s$. Thus,

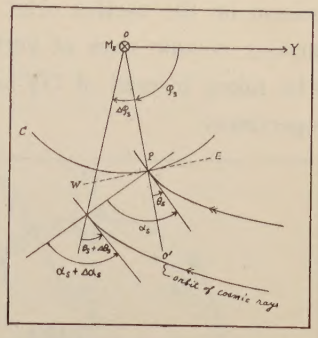

Fig. 3 Arc C is the earth's orbit and P is the position of earth. Axes and symbols used in the paper are shown.

$$\frac{d\alpha}{dx}=\frac{d\theta_s}{dx}-\frac{d\varphi_s}{dx}=\frac{d\theta_s}{dx}-\frac{\cos\theta_s}{r_s}$$

$$\therefore\quad \Delta\alpha\simeq\Delta\theta_s-\cos\theta_s\cdot\frac{\Delta x}{r_s} \qquad (2)$$

On the other hand, from $\sin\theta_s=\frac{r}{r_s}-\frac{1}{r_s^2}$,

$$\Delta(\sin\theta_s)\simeq\frac{d(\sin\theta_s)}{dx}\Delta x=\left\{\frac{dr}{dx}+\left(-\frac{r}{r_s}+\frac{2}{r_s^2}\right)\sin\theta_s\right\}\cdot\frac{\Delta x}{r_s} \qquad (3)$$

Thus, except the case that $\frac{dr}{dx}$ is considerably large, $\Delta\alpha$ is the order of $\frac{\Delta x}{r_s}$. If we take fifty times earth's radius for Δx, which is considered to be region for cosmic rays being effectively influenced by the earth's magnetic field, $\frac{\Delta x}{r_s}$ is 2.1×10^{-4} and so $\Delta\alpha$ is negligible small. Thus, cosmic rays are incident into effective region of earth's magnetic field in a parallel beam approximately. Furthermore, if we take usual dimension of cosmic-ray meter for Δx in the case of deflection of cosmic rays by the earth's magnetic field, $\Delta\alpha$ is negligible small in this case also and cosmic rays are incident upon the erath in a parallel beam approximately. Thus, in the case that deflections of cosmic rays by the sun's and the earth's magnetic field are taken into account together, intensity distribution of cosmic rays on the earth in a certain season is such as the part corresponding to outer orbit in Fig. 2, but its relative magnitude changes with season in such a manner as shown in Fig. 2 also.

Next, at the limit of increasing intensity in Fig. 2, $j(\varphi_s)$ tends to ∞ due to increasing of $\frac{\partial r}{\partial\varphi_s}$ towards ∞. Although this divergence is merely mathematical and integral intensity $\int_0^{\Delta x}j(\varphi_s)\,dx=\int_0^{\Delta x}\left|\frac{dr}{dx}\right|dx=\int_0^{\Delta r}dr$ is finite, the intensity is very strong at this point. But, at the same time, the angle θ_s of incidence of cosmic rays changes very largely near this point, as known from equation 3. Intensity problem in such case cannot be treated simply and was omitted out of the present consideration. However, it is only small region of φ_s to be excluded for this reason.

Now, the dependence of angle $\theta_s(\varphi_s)$ of incidence of cosmic rays upon φ_s is given by Fig. A2 of appendix 1. From Fig. 2 and Fig. A2, we can express the intensity of cosmic rays at each point of the earth's orbit with its direction of incidence expressed in solar time on harmonic dial. They are shown in Fig. 4 a, 4 b and 4 c. There, two full lines correspond to two branches with different directions of incidence of cosmic rays as seen in Fig. 2 and dotted line is vector sum of these two branches. The

position on the earth's orbit is shown by angle φ_s written on the curves. When we consider cosmic rays of vertical incidence on the earth, OY′-axis and OY″-axis ought to be taken instead of OY-axis in the cases of $M_s=10^{34}$ and $M_s=2.5\times10^{33}$ gauss cm^3, respectively.

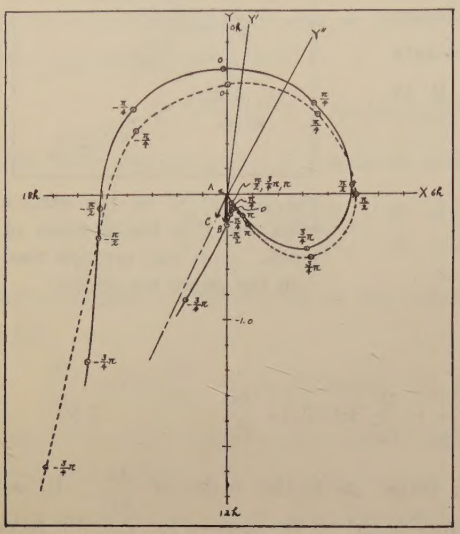

Fig. 4 a For $r_s=4$ Störmer of cosmic-ray energy, intensity of cosmic rays at each point of earth's orbit with its direction of incidence are reproduced on harmonic dial. In the case that cosmic rays incident vertically on the earth are considered, axis OY′ and OY″ are to be taken for o-hour axis instead of OY in the case of $M_s=10^{34}$ and 2.5×10^{33} gauss cm^3, respectively. Two full lines correspond to two branches with different directions of incidence of cosmic rays as seen in Fig. 2 and dotted line is vector sum of these two branches. Vector A, B, and C are resultant vectors of two branches mentioned above and their vector sum.

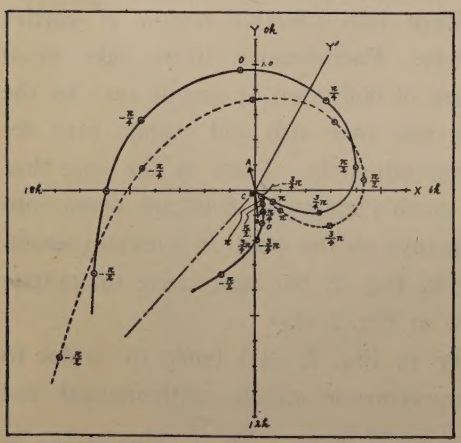

Fig 4 b It is the same figure for $r_s=2$ Störmer as Fig. 4 a.

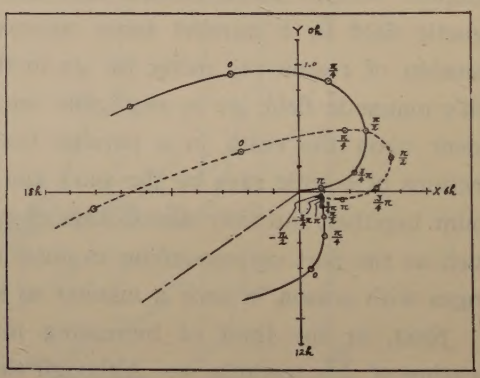

Fig. 4 c It is the same figure for $r_s=1$ Störmer as Fig. 4 a.

Furthermore, vector A, B and C are resultant vectors of above two branches and their vector sum. In the case of $M_s=10^{34}$ gauss cm^3, $r_s=4$ and 2 Störmer of cosmic-ray energy correspond to $r_e=2$ and 1 Störmer, respectively. Then, mean intensities of $r_e=2$ and 1 Störmer of cosmic-ray energy given by resultant vectors C are about 1/5 and 1/25 of intensity at infinity, respectively. That is, mean intensity averaged over all season never tends to zero due to the general magnetic field of the sun, as mentioned at the beginning of this paper.

The author wishes to express his cordial thanks to professor Y. Sekido for his suggestion of the problem and his guidance throughout this work.

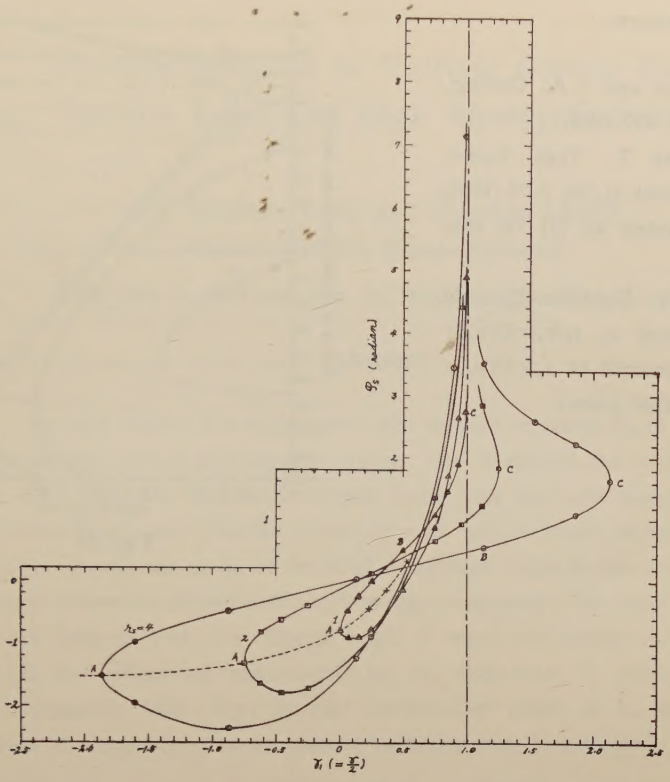

Fig. A1a

APPENDIX

1. In Fig. A1a and A1b, angle φ_s is plotted against γ_1, taking r_s for parameter. The parts A–B–C of curves correspond to outer orbit. In Fig. A2, angle θ_s is plotted against φ_s, taking r_s for parameter.

2. At the point where $\frac{\partial \gamma}{\partial \varphi_s} \to \infty$, that is, $\frac{\partial \varphi_s}{\partial \gamma}=0$, $\frac{\partial \varphi_s}{\partial \theta_s}=0$. Furthermore, $\frac{\partial x_s}{\partial \theta_s}=\pm 1$ (+: inner orbit, −: outer orbit) and thus $\frac{\partial t_a}{\partial t_e}=0$, as seen from equation (1), (2) and equations in appendix of the paper [1]. It should be noticed that the point in Fig. 2 where $j(\varphi_s)\to\infty$ corresponds to the point in Fig. 4 of [1] where $\frac{\partial t_a}{\partial t_e}=0$.

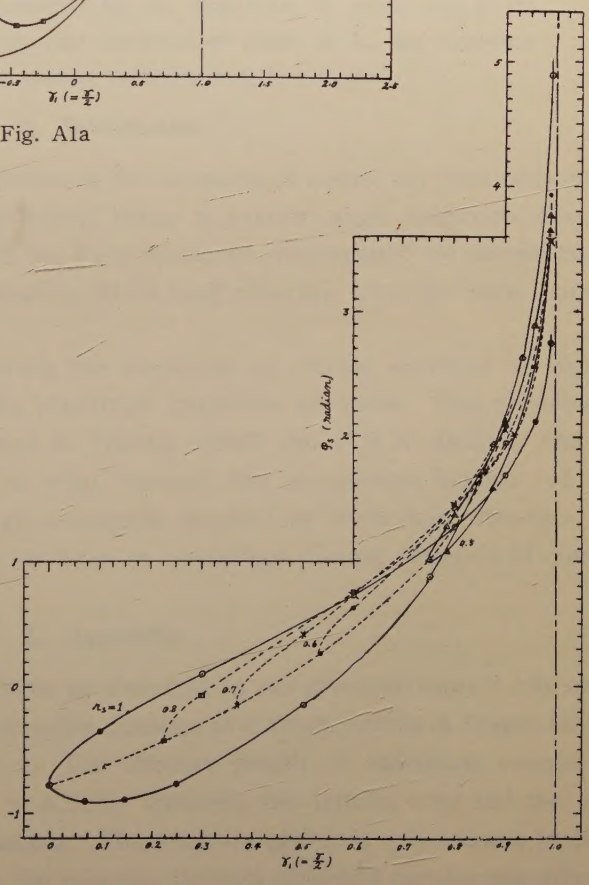

Fig. A1b

References

[1] A.H. Compton and I. A. Getting, phys. Rev. **47**, 817 (1935).

[2] Y. Sekido and T. Yagi, Journ. Geomag. Geoelect. II, No. 3, 78 (1950), which is denoted as [1] in this paper.

Erratum in [1] : Equation (2) ought to be corrected as $r_s/r_e = D/a_e \times (M_e/M_s)^{1/2}$, instead of $r_s = D/a_e \times (M_e M_s)^{1/2}$ in that paper.

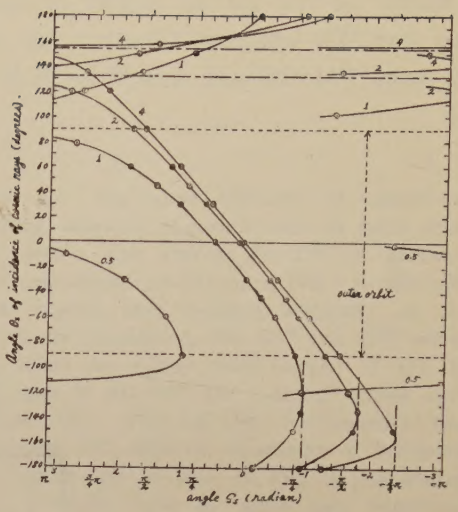

Fig. A2

Diurnal Variation of Vertical Cosmic Rays ——Narrow Total and High Energy Components

By Teiichiro YAGI and Hiroyuki UENO
Physical Institute, Nagoya University

(Read May 6, 1955 and May 14, 1956; Received Oct. 1, 1956)

Abstract

It is well known that anomalous solar diurnal variation S_D of cosmic rays appears at the time of geomagnetic storms. We confirmed the existence of S_D about the cosmic-ray intensities of total component and high energy component penetrating 90 cm lead absorber measured with narrow angle telescope directed vertically. Amplitude of S_D of the total component is the largest and the time of maximum intensities of that of the high energy component is the latest. The phases of S_D are different with five different kinds of cosmic-ray meters in our country. This can be understood qualitatively by the deflections of cosmic rays in the earth's magnetic field. Year to year variation of phase of S_D and long-time variation of amplitude of mean diurnal variation were investigated.

1. Introduction

Since 1949, continuous observation of the intensities of cosmic ray total component has been carried out in our laboratory, using a narrow angle telescope directed vertically. Furthermore, since 1952, we have measured continuously the intensities of the high energy component penetrating 90 cm lead absorber, with the same narrow angle telescope directed vertically.

When geomagnetic storm occurs, the amplitude of diurnal variation of cosmic rays increases and the time of its maximum intensities advances. This phenomena were already found by Y. Sekido and S. Yoshida (1950) and D.W.N. Dolbear and H. Elliot (1951).[1] We investigated in what manner this phenomena happen for the cosmic-ray intensities of high energy component penetrating 90 cm lead absorber. In connection with this result, some features of anomalous diurnal variation of cosmic rays were reexaminend.

2. Apparatus

The apparatus is almost the same as described in our previous paper,[2] but some alterations are as follows. The telescope consists of 4 trays, having 6 Geiger-Müller counters in each, as shown in Fig. 1. The effective length of individual counter is 28 cm and the effective diameter is 4.5 cm. Between the bottom tray and the tray above it, 90 cm lead absorber is inserted. The numbers of 3 fold coincidences (a, b, c) and (b, c, d) are recorded in every ten minutes, through scale-of-4 circuits respectively.

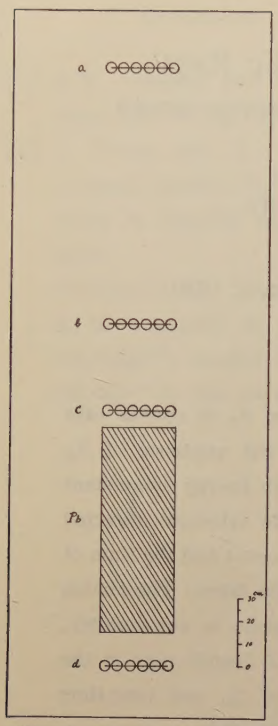

Fig. 1 Front view of apparatus

The maximum zenithal angles of incident cosmic-ray particles causing these 3 fold coincidences are both 12 degrees, their averaged numbers per hour are 174×4 and 87×4, and their statistical fluctuations of hourly values are 3.7% and 5.4%, respectively. The minimum momentum of cosmic-ray particles causing 3 fold coinciences (b, c, d) is 1.3 Gev/c for μ mesons, owing to their penetration of 90 cm lead. Also, the numbers of 2 fold coincidences (b, c) are recorded in every minute, through a scale-of-16 circuit. The corresponding values of them are 40 degrees, 618×16 particles per hour, and 0.98%, respectively. In the following, we will denote T (narrow angle, total), H (narrow angle, high energy) and W (wide angle, total) for 3 fold coincidences (a, b, c), (b, c, d) and 2 fold coincidence (b, c), respectively, in abbreviation.

3. Barometer effect and mean diurnal variation

3—1. Barometer effect The barometric pressure was observed at Nagoya District Meteorological Observatory, 16 times a day till December, 1952, and 8 times a day thereafter. The heights of isobar levels of upper atmosphere were obtained from the radio-sonde data, observed at Shionomisaki Meteorological Observatory, about 210 km SSW apart from Nagoya, and at Wajima Meteorological Observatory, about 240 km N apart from Nagoya, at about 0-h and 12-h every day.

On the daily means of cosmic-ray intensities I, barometric pressures P, the difference of heights of isobar levels between 100 mb and 1000 mb H_1, and the difference of heights of isobar levels between 100 mb and 200 mb H_2, we take departures of daily means from their 27-day running averages and then average these departures over 3 days. Using such means of each element over every three days, 4-fold multiple correlations were computed to study the atmosperic effect. The whole period, June 1952—July 1955, among which the data were used in the analysis, was devided into four period, covering from 7 months to 12 months and four calculations were carried out for these four periods. Stillmore, one calculation was carried out for the last period, using only

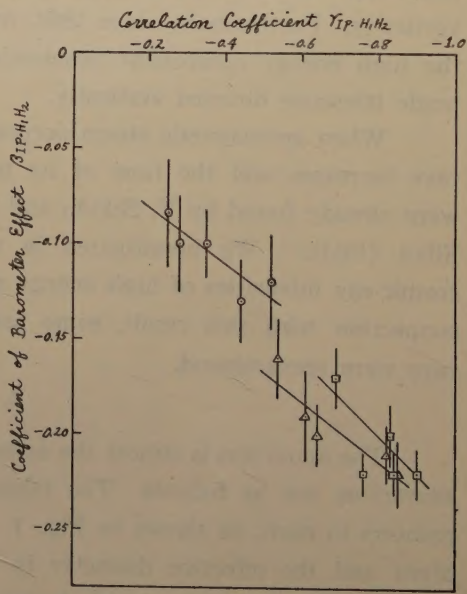

Fig. 2 Coefficients of barometer effect are plotted against correlation coefficients.
⊙ : H △ : T ⊡ : W

such materials that barometric pressures deviate more than standard deviation of them.

The coefficients of barometer effect $\beta_{IP\cdot H_1H_2}$ thus obtained are plotted against the corresponding correlation coefficients $\gamma_{IP\cdot H_1H_2}$ in Fig. 2. From this, such tendency is to be seen that the larger the correlation coefficients, the larger the coefficients of barometer effect become. So we adopt the value of coefficient of barometer effect corresponding to maximum correlation coefficient:

$$\beta_H = -0.13\%/\text{mb} \qquad (H)$$
$$\beta_T = -0.22\%/\text{mb} \qquad (T)$$
$$\beta_W = -0.22\%/\text{mb} \qquad (W)$$

But, throughout the present analysis, we have applied $\beta_H = -0.15\%/\text{mb}$ for H, obtained in the preliminary analysis at the first stage and $\beta_T = -0.24\%/\text{mb}$ and $\beta_W = -0.19\%/\text{mb}$ for T and W respectively, reported in our previous paper.[2] Hewever, these difference is not so significant that the following results on the cosmic-ray diurnal variations may be changed qualitatively. For example, the semiamplitude of 1st harmonic of solar diurnal variation of barometric pressure, averaged in a year, June 1952—May 1953, amounts to 0.7 mb, which gives only the difference of correcting values less than 0.02%, corresponding to the difference of coefficients of barometer effect mentioned above. On the other hand, not so reliable values of coefficients of temperature effects $\alpha_{IH_1\cdot PH_2}$ and $\gamma_{IH_2\cdot PH_1}$ were obtained.

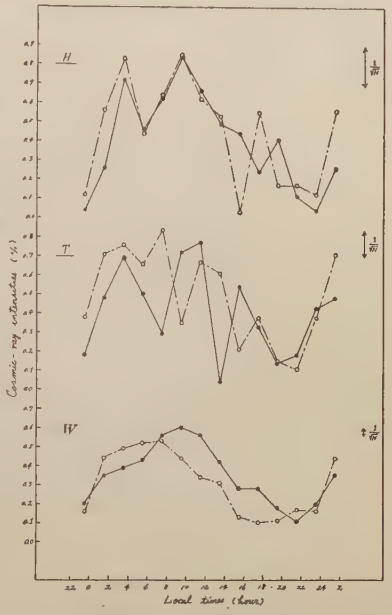

Fig 3. Diurnal variations of bihourly cosmic-ray intensities corrected for barometer effect averaged over a year.
●—●: June 1952—May 1953
○—○: June 1953—May 1954

3–2. Mean solar diurnal variation of cosmic rays. The solar diurnal variations of cosmic-ray intensities averaged over a year are reproduced in Fig. 3, after being corrected for barometer effect. In the year, June 1952—May 1953, the total numbers of days were 315, 314, and 287 for H, T and W, respectively. In the year, June 1953—May 1954, they were 332, 337 and 311 for H, T and W respectively.

The 1st harmonics of these mean solar diurnal variations are shown on a harmonic dial in Fig. 4a. Fig. 4b shows the result of their means taken over those two years, giving also that of low energy component (L) with the range less than 90 cm lead which was obtained by subtracting H from T. From this result, the phase differences between T, H and L are as follows:

$\Delta\Psi(T, H) = 30.8 \pm 16.6$ degrees between T and H
$\Delta\Psi(L, T) = 41.4 \pm 21.1$ „ „ L „ T
$\Delta\Psi(L, H) = 72.2 \pm 22.0$ „ „ L „ H

If we were, at the present, allowed to disregard the difference of temperature effect between the different components, these phase differences would be attributed to the differences of the deflections of primary cosmic rays in the earth's magnetic field,

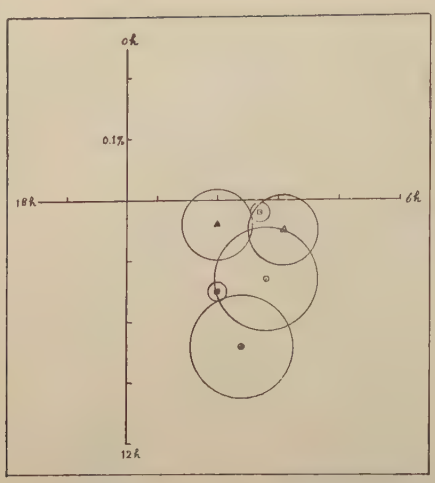

Fig. 4a 1st harmonics of cosmic-ray diurnal variations are plotted on a harmonic dial.

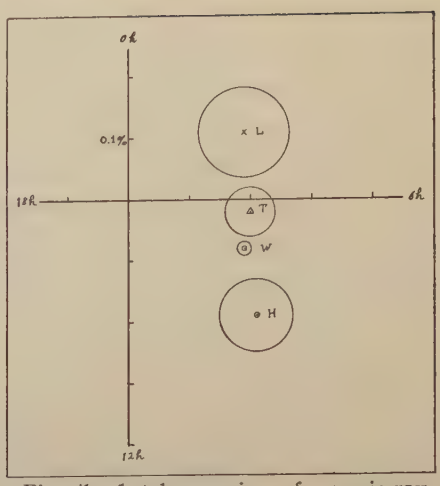

Fig. 4b 1st harmonics of cosmic-ray diurnal variations averaged over June 1952—May 1954 are plotted on a harmonic dial.

	June 1952—May 1953	June 1953—May 1954
H	●	○
T	▲	△
W	■	□

depending on the mean energies of different components. According to E. Brunberg,[3] the mean energy of total components of cosmic rays as giving rise to solar diurnal variations amounts to 21 ± 5 Gev, which was measured with narrow angle telescope inclined 30 degrees to the zenithal direction. If we assumes for mean energy of total components of cosmic rays T as causing solar diurnal variation to be 21 Gev also, though they are measured with narrow angle telescope directed vertically, the above described phase difference gives the mean evergies of L and H to be $14.5\pm\frac{2.2}{1.4}$ Gev and $39\pm\frac{30}{13}$ Gev, respectively. This mean energy of L will support the discussion in a subsequent section 4–2.

4. Anomalous solar diurnal variation S_D associated with geomagnetic storms

4–1. Statistical method. The data used in this analysis were obtained by the five different kinds of cosmic-ray meters in Japan, whose descriptions and notations were given in Table I. To avoid from the confusion owing to the latitude effect and the longitude effect of cosmic-ray diurnal variation, we confined ourselves to the data observed in our country. The period in which the data were used was two years, June 1952—May 1954, in which 37 cases of geomagnetic storms were reported by Kakioka Geomagnetic Observatory.

Intensities of cosmic rays often decrease suddenly at the time of occurrence of geomagnetic storms and these worldwide changes of intensities may appear in the rusults of analysis as if diurnal variation, for the sake of curvature effect. In order to avoid this effect approximately, we treated the departures of hourly values from

their 24-hour running averages and diurnal harmonics were treated conveniently.

Table I

Notation	Location of observatory	Apparatus			Numbers of storms adopted			
			absorber	aperture	*TO*	*S*1	*S*2	*r*
T	Nagoya University	counter telescope	no.	±12°	34	15	25	22
H	,,	,,	90cm Pb	±12°	34	15	25	22
W	,,	,,	no.	±40°	34	16	25	22
*N*3	the Scientific Research Institute at Tokyo	,,	no.	±85°	31	13	21	21
NI	,,	ionization chamber	10cm Pb	±90°	37	17	27	25

Taking the day of occurrence of each geomagnetic storms as the Oth day, we denote S_b for the mean diurnal variation averaged over 3 days before the occurrence of geomagnetic storm (from −3rd to −1st) and S_a for the mean diurnal variation averaged over 3 days after that (from +1st to +3rd). We difine not S_a, but $\vec{S}_D=\vec{S}_a-\vec{S}_b$ as the anomalous diurnal variation associated with geomagnetic storm. Such definition was also adopted by S. Yoshida[4] in her analysis.

4-2. Results. The mean S_D averaged over all storms are shown on harmonic dial in Fig. 5a.–Fig. 5d, to which suffices "*To*" are attached. From this it is to be seen that vectors S_D of different instruments point out different directions. In order to confirm whether these differences of directions are due to statistical fluctuations or not and whether they depend upon the selections of group of storms or not, following analysis were carried out.

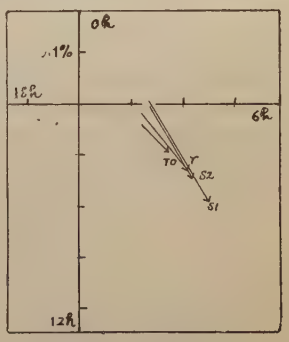

Fig. 5a S_D of $N3$

At first, $N3$, having been observed by the group of the Scientific Research Institute is the cosmic-ray intensities

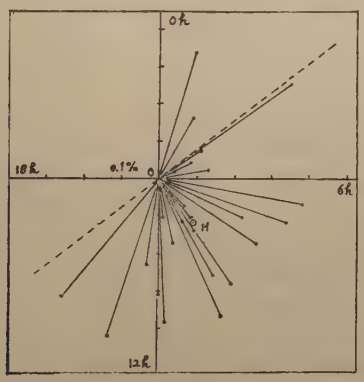

Fig. 6b Each S_D of $N3$ calculated on such geomagnetic storms in June 1952—May 1954 that $r_a-r_b>0$ are plotted on a harmonic dial. The total numbers are 25, including 4 of *NI*. OM is mean S_D vector.

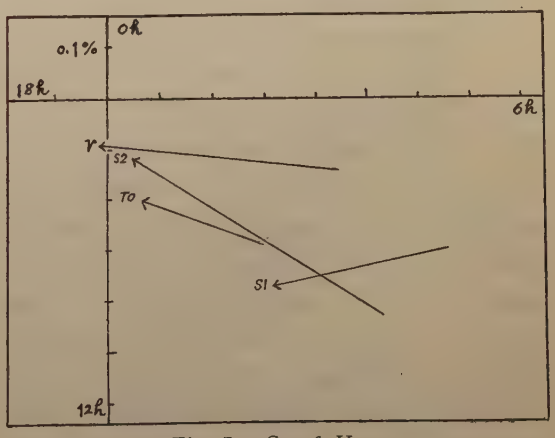

Fig. 5c S_D of H

with the highest accuracy in our country and the statistical fluctuation of its hourly value amounts to only 0.26%. So that, we calculated S_D of each storm observed by $N3$, which are shown in Fig. 6a. In this figure, dividing the plane into two half planes by the straight line L through original point and perpendicular to the mean S_D vector OM, such cases that the end points of S_D exist in the half plane including the point M are 27 (73%) and the other cases are 10 (27%). That is, we should give attention to the following facts as one charactor of S_D, "The dispersion of the directions of S_D of individual storms is very large, but the most of their directions are inside ± 90 degrees from the direction of mean S_D."

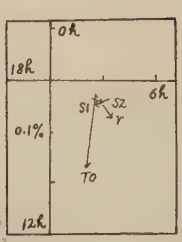

Fig. 5d S_D of NI

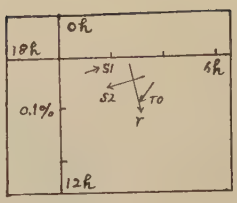

Fig 5e. S_D of W

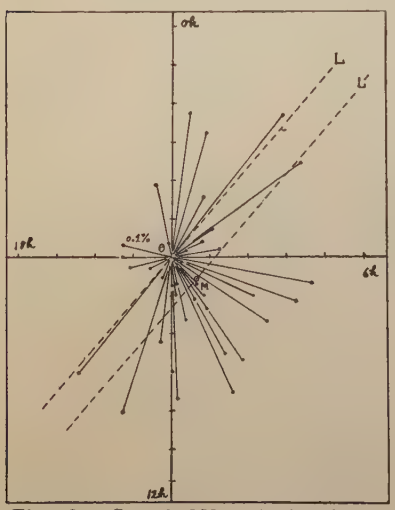

Fig. 6a S_D of $N3$ calculated on individual geomagnetic storms in June 1952—May 1954 are plotted on a harmonic dial. The total numbers are 37, including 6 of NI. OM is mean S_D vector.

Next, we computed the mean S_D about the following groups of geomagnetic storms, on the basis of each S_D of every storms mentioned above:

"$S1$": dividing into two half planes by the straight line L' through M perpendicular to OM, group of such storms that the end points of S_D of $N3$ exist in the half plane not including O.

"$S2$": among two half planes divided by straight line L, group of such storms that the end points of S_D of $N3$ exist in the half plane including M.

"r": denoting r_a and r_b for the amplitudes of S_a and S_b respectively, group of such storms that $r_a - r_b > 0$, that is, the amplitudes of diurnal variation increase at the time of geomagnetic storms. (refer to Fig. 6b.)

The mean S_D about these groups are shown in Fig. 5a—Fig. 5d also, to which corresponding suffices are attached. As seen in these figures, S_D observed with a certain instrument point out almost the same direction, inspite of the different ways of selecting the storms. (But this tendency is not so clear for W and NI, because their accuracies are low. For T and H, it is rather

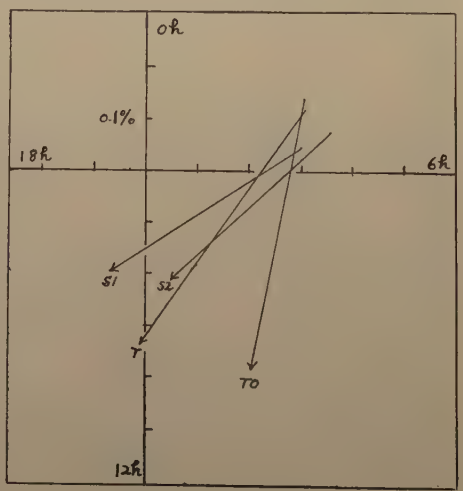

Fig. 5b S_D of T

clear, because diurnal variations observed with narrow angle telescopes are large, though their accuracies are low. It is most clear for $N3$ because its accuracy is the highest.)

These S_D vectors are reproduced in Fig. 7, gathered together into the original point. Also, the times of maximum intensities and the amplitudes of mean S_D for the group "*To*" and the group "γ" are shwon in Fig. 8a and Fig. 8b. From Fig. 7, Fig. 8a and Fig. 8b, the following facts can be recognized, although the errors are large.

(a) Ampitude. The ratio of amplitude of S_D observed with narrow angle telescope directed vertically (T) to that observed with wide angle telescope (W, $N3$, NI) is about "factor 5." One reason of this is that wide angle telescope measures cosmic rays incident from different

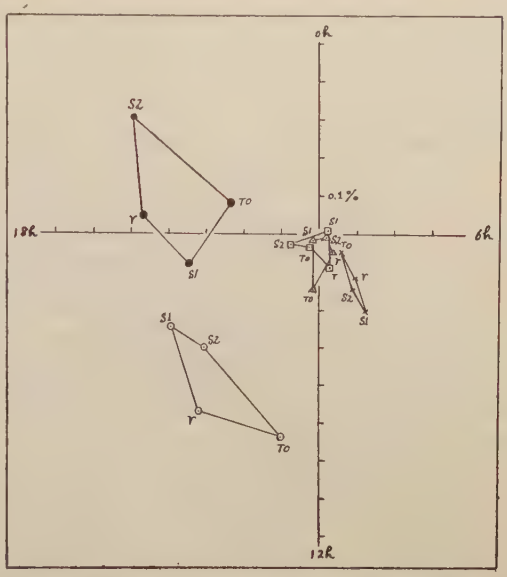

Fig. 7 S_D of several kinds of cosmic-ray meters calculated on geomagnetic storms in June 1952—May 1954 are plotted on a harmonic dial.
●: H, ○: T, □: W, ×: $N3$, △: NI.

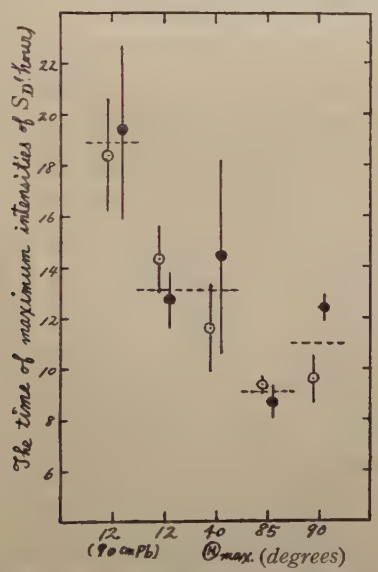

Fig. 8a The times of maximum intensities of S_D are plotted against the maximum semiangles of telescopes. ●: "TO"; mean averaged over all storms. ○: "γ"; mean averaged over such storms that $r_a - r_b > 0$ about the data of $N3$.

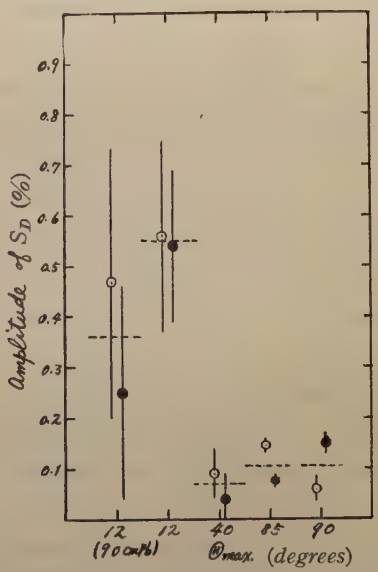

Fig. 8b The amplitudes of S_D are plotted against the maximum semiangles of telescopes. ●: "To"; mean averaged over all storms. ○: "γ"; mean averaged over such storms that $r_a - r_b > 0$ about the data of $N3$.

directions at the same time, so that the amplitude of diurnal variation measured with it becomes small for the "average effect." The other reason is that cosmic rays measured with narrow angle telescope directed vertically pass through smaller mass of atmosphere and thus contain more contributions from low energy primaries.

(b) The time of maximum intensities.

(i) Narrow angle telescope: The time of T is earlier than that of H.

(ii) Wide angle telescope: The time of $N3$ is earlier than that of NI.

(iii) Narrow angle telescope and wide angle telescope: The time of $N3$ is earlier than that of T.

These facts can be explained qualitatively as follws. Let us assume that anisotropic flux of cosmic rays exists far outside the earth's magnetic field and causes cosmic-ray diurnal variation as observed on the rotating earth, then the time of maximum intensities of diurnal variation depends upon the mean energy of cosmic rays observed, owing to their deflections in the earth's magnetic field. The lower the mean energy of cosmic rays, the earlier the time of maximum intensities becomes for the primaries of positive charge. Thus (i) is evident. (ii) For $N3$ is more directional than NI, $N3$ measures the cosmic rays of lower energies than NI. (iii) According to E. Brunberg's figures[5] on the deflection of cosmic rays in the magnetic dipole field, Ψ_E which gives the change of longitude of particle's position is not symmetrical to zenithal direction. The difference of Ψ_E between direction inclined north and zenithal direction is larger than that between zenithal direction and direction inclined south. And in the region of low energy, the difference of Ψ_E between direction inclined east and zenithal direction is larger than that between zenithal direction and direction inclined west. (For the case of latitude $\lambda_m=25$ degrees and momentum $p=30$ Gev/c, $\Psi_E(48°\mathrm{N})-\Psi_E(0°)=33°$, $\Psi_E(0°)-\Psi_E(48°\mathrm{S})=5°$; $\Psi_E(48°\mathrm{E})-\Psi_E(0°)=60°$, $\Psi_E(0°)-\Psi_E(48\mathrm{W}°)=40.°$) Thus, the mean Ψ_E of cosmic rays measured with wide angle telescope directed vertically is larger than that of cosmic rays measured with narrow angle telescope directed vertically, so the time of maximum intensities of cosmic-ray diurnal variation measured with the former is earlier than that of the latter.

In such a way, the difference of times of maximum intensities of S_D measured with different instruments can be explained qualitatively by the difference of deflections of cosmic rays in the earth's magentic field, depending on the mean energies. But the exact quantitative treatment of this result is impossible for the present, because the overall multiplicities of cosmic rays incident from inclined directions are not well known. Finally, we should refer to the fact that the relation between the anomalous diurnal variation of total component (T) and that of high energy component (H), measured with narrow angle telescope directed vertically, became clear for the first time, when we defined $\vec{S}_D=\vec{S}_a-\vec{S}_b$ as the anomalous diurnal variation associated with geomagnetic storms.

4–3. Interpretation of the rusult of narrow angle telescope directed vertically

Especially we will consider the result of narrow angle telescope directed vertically among the results of S_D explained in the subsection 4–1, because the quantitative

treatment of them is more simple than the others. Fig. 9 shows the differential effective primary spectrum calculated by K. Nagashima,[6] that is, the intensities of total components of vertical cosmic rays $i(E, x_0)$ produced by the primary cosmic rays of kinetic energy E at the atmospheric depth $x_0 = 10\ mH_2O$. Curve I and II correspond to two limiting cases. In the same figure, the deflections of primary cosmic rays in the earth's dipole field are reproduced from E. Brunberg's figures.[5] For T, we take magnetic cut-off energy in Japan, geomagnetic latitude 25°N, as 10 Gev. Next, we must determine the effective primary spectrum of high energy cosmic rays H. The effective primary spectrum shown in Fig. 9 was computed on the ground of latitude effect only and there is not significant difference of latitude effect of vertical cosmic rays between total component and hard component.[7] Therefore, we assume that the shape of effective primary spectrum of hard component is the same as that of total component shown in Fig. 9, with the exception of the difference of absolute flux. Taking the intensity of T as 100%, the intensities of hard component and H are 70% and 50%, respectively. Thus, 20/70=29% of hard component are absorbed by the 90 cm lead. So that, in Fig. 9, we draw the inclined straight line from the point of $E=10$ Gev in such a way that the low energy part of curve cut off by this line amounts to 29% of total intensity. Now we can consider the high energy part as the effective primary spectrum of H.

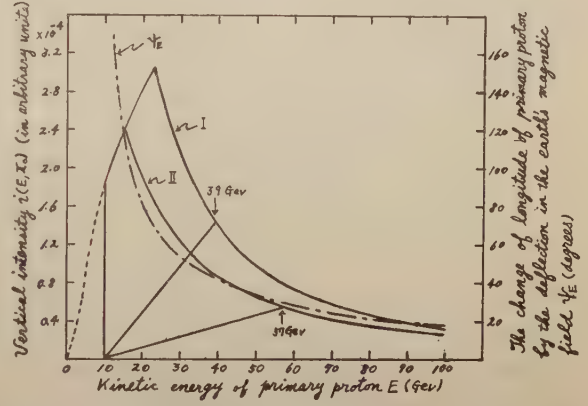

Fig. 9 Differential effective primary spectrum $i(E, x_0)$ at sea level is plotted against kinetic energy E of primary proton. Curve I and II correspond to two limiting cases. (after K. Nagashima) The change of longitude of particle's position by the deflection in the earth's magnetic field is reproduced in the same figure. (after *E.* Brunberg)

Here, according to T.H. Johnson,[7] it is known that latitude effect and east-west effect of cosmic rays vanish at the depth of 16 mH_2O, namely, field sensitive rays of primary energies from 7 Gev to 14 Gev are absorbed at that depth. On the other hand, 90 cm lead is just equivalent to 6 mH_2O of air for the range of μ meson. Thus, almost all of secondary particles produced by primary cosmic rays of energies from 10 Gev (cut-off energy) to 14 Gev are absorbed by 90 cm lead. This is the reason why we draw the inclined straight line in such a way that the part of low energy is absorbed in order to determine the effective primary spectrum of H. Also, we have seen in subsection 3–2 that the mean energy of low energy component L defined as the difference between T and H is about 14.5 Gev. This result supports above consideration too.

Let us assume that anisotropic flux of cosmic rays is formed far outside the earth's magnetic field by any mechanism of acceleration in a certain direction, by

which cosmic rays obtain a gain of energy ΔE Gev. Then, as K. Nagashima[8] pointed out at the first time, the change of intensities are:

$$\Delta i(E\ x_0)=\Delta E\cdot\left\{\frac{2}{3}\cdot\frac{1+4aE^{\frac{4}{3}}}{E(1+aE^{\frac{4}{3}})}+\frac{2(E+m_0)}{(E+m_0)^2-m_0^2}\right\}\cdot i(E,\ x_0)\,, \qquad (1)$$

$a=00.9$, constant number

$m_0=0.93$ Gev, rest energy of proton,

where the terms of orders higher than $(\Delta E)^2$ are neglected and the primary spectrum obtained by H.V. Neher[9] was used. The first term in bracket arises from the shift of energy spectrum and the second term arises in connection with Liouville's theorem.

Taking the space distribution of anisotropic flux as $A_0=\Delta i(E,\ o)\ \cos(\Psi)$ and denoting the change of longitude of particle's position by the deflection in the earth's magnetic field as $\Psi_E(E)$, diurnal variation on the earth is:

$$A=\int_{E_c}^{\infty}\Delta i(E,\ x_0)\cos\{\Psi-\Psi_E(E)\}dE\Big/\int_{E_c}^{\infty}i(E,\ x_0)dE$$

$$=A(E_c)\cos\{\Psi-\Psi_E(E_c)\}$$

$$A^2(E_c)=\left\{\int_{E_c}^{\infty}\Delta i(E,\ x_0)\cos\Psi_E(E)dE\right\}^2+\left\{\int_{E_c}^{\infty}\Delta i(E,\ x_0)\sin\Psi_E(E)\,dE\right\}^2\Big/\int_{E_c}^{\infty}i(E,\ x_0)dE\,,$$

$$\tan\Psi_E(E_c)=\int_{E_c}^{\infty}\Delta i(E,\ x_0)\sin\Psi_E(E)\,dE\Big/\int_{E_c}^{\infty}\Delta i(E,\ X_0)\cos\Psi_E(E)dE\,. \qquad (2)$$

Taking $\Delta E=6\times10^{-6}$ Gev, the results caculated from eq. (1) and eq. (2) are given in Table II. It gives 24~26 degrees as the difference of phase of diurnal variation between T and H. On the other hand, from Fig. 7 and Fig. 8a, the phase difference of S_D between T and H is about 60~90 degrees, which is considerably larger than the calculated one, although the experimental error is large.

Table II

	Amplitude $A\ (E_c)$ %		Phase $\Psi_E(E_c)$ degrees		Mean energy corresponding to $\Psi_E(E_c)$ Gev	
	I	II	I	II	I	II
A_0	18.7		0		—	
T	0.50	0.54	67.0	61.9	21	25
H	0.36	0.35	41.3	38.3	41	44

5. S_D in different years

In order to see year to year variation of S_D, we calculated each S_D of $N3$ about each geomagnetic storm, which was observed at Kakioka Geomagnetic Observatory among the period from July 1947 to May 1954, by the same statistical method as mentioned in subsection 4–1.

Each S_D of such geomagnetic storms that $r_a-r_b>0$, that is, the amplitudes of diurnal variations of cosmic rays increase at the time of geomagnetic storms are plotted

on a harmonic dial in Fig. 10a. Frequency distribution of the time of maximum intensities of those is shown in Fig. 10b. The time of maximum intensities of mean S_D is 9.5 hour in local time.

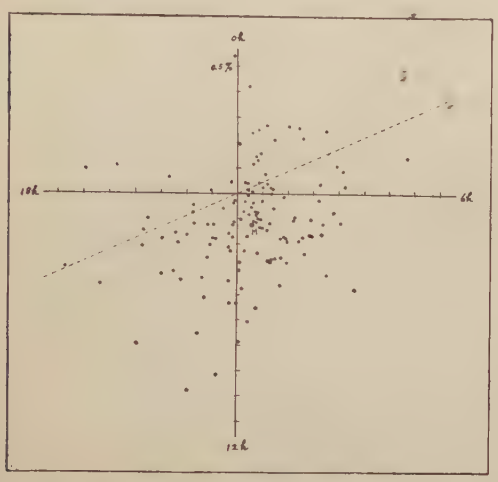

Fig. 10a Each S_D of $N3$ calculated on such geomagnetic storms in July 1947—May 1954 that $r_a - r_b > 0$ are plotted on a harmonic dial. OM is mean S_D vector.

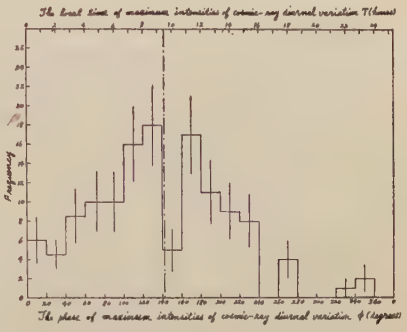

Fig. 10b Frequency distribution of the time of maximum intensities of each S_D of $N3$ calculated on such geomagnetic storms that $r_a - r_b > 0$.
——·—— ·: Mean

Next, we calculated S_D in every year averaged on such geomagnetic storms that the amplitudes of diurnal variations increase and the ranges ΔH of horizontal force exceed 100γ respectively. They are shown in Fig. 11a and Fig. 11b. The numbers of geomagnetic storms in each case are given in Table III. From these, it is to be

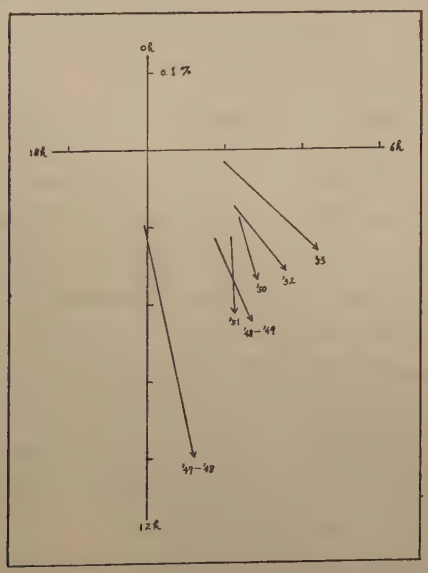

Fig. 11a S_D of $N3$ in every year averaged on such geomagnetic storms that $r_a - r_b > 0$ are plotted on a harmonic dial.

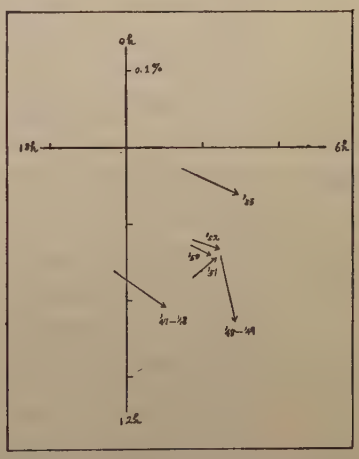

Fig. 11b S_D of $N3$ in every year averaged on such geomagnetic storms that $\triangle H > 100\gamma$ are plotted on a harmonic dial.

seen that S_D in every year point out about a definite direction and shift their position (S_h) from year to year. The movement corresponds to the change of phase of cosmic-ray diurnal variation with 22-year's cycle found by T. Thambiyahpillai and H. Elliot.[10] Thus S_h, namely, S_q after S. Yoshida[4] is considered to consist mainly of component of secular variation on the average.

Table III

Classification / Period	The numbers of geomagnetic storms		
	$\Delta H > 100\gamma$	$r_b - r_a > 0$	Total
Jul., 1947—Jun., 1948	12	19	31
Jul., 1948—Jun., 1948	26	36	54
Jan., 1950—Dec., 1950	24	18	42
Jan., 1951—Dec., 1951	23	24	46
Jan., 1952—Dec., 1952	21	20	30
Jan., 1953—Dec., 1953	13	12	18
Jan., 1954—May., 1954	0	1	2
77 months	119	130	223

This result leads us to the following physical picture. Anisotropy S_q is already formed in a large space around the sun in a long range from the earth. At the time of geomagnetic storm, the earth is immersed in a perturving medium, thrown out from the sun and generating geomagnetic storm. Then cosmic rays are accelerated when passing through the perturving medium, and anisotropy S_D is formed in the neighbourhood of the earth. So we observe the resultant of S_q and S_D at the time of geomagnetic storm.

6. Long-time change of diurnal variation of cosmic rays

12 months' averages of first harmonics of cosmic-ray diurnal variations were computed in every month, using the data of T and W from March 1949 to February 1956 and the data of $N3$ from January 1950 to August 1955. (Among these series, the observation of T from October 1951 to May 1952, that of W from October 1951 to February 1952, and that of $N3$ from July to December 1949 were interrupted.) The amplitudes and the phases of them are reproduced in Fig. 12a and Fig. 12b. At the same time, 12 months' averages of K-index (monthly mean of daily sum reported by Kakioka Geomagnetic Observatory) and those of relative sunspot number (monthy mean, among which recent data were those reported by Tokyo Astronomical Observatory) were computed in every month, which are shown in Fig. 13.

From this, it is to be seen that the amplitudes of cosmic-ray diurnal variations increase from 1951 to 1952 and this increase is much larger for T than for W and $N3$. Further, it should be noticed that at about the same time K-index shows remarkable increase. On the contrary, relative sunspot number does not show such remarkable

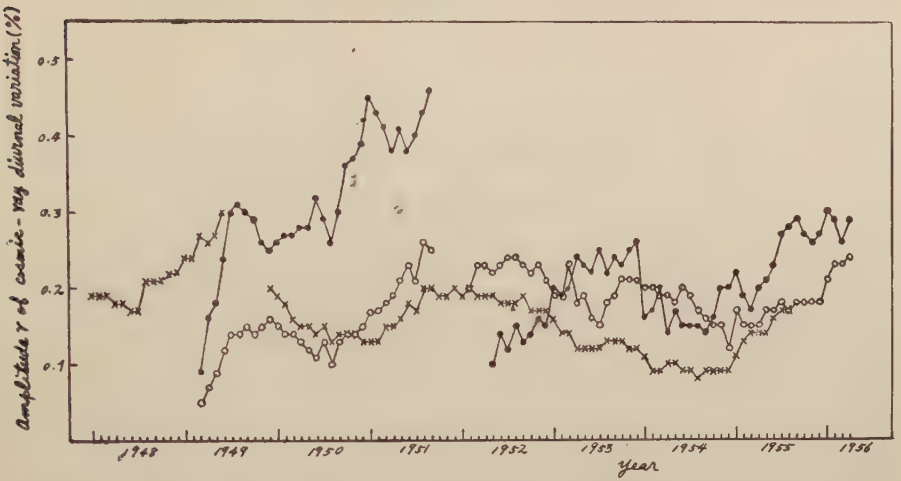

Fig. 12a The amplitudes of 12 months' averages of 1st harmonics of cosmic-ray diurnal variations are plotted in every month.
●—●: T, ○—○: W, ×—×: $N3$

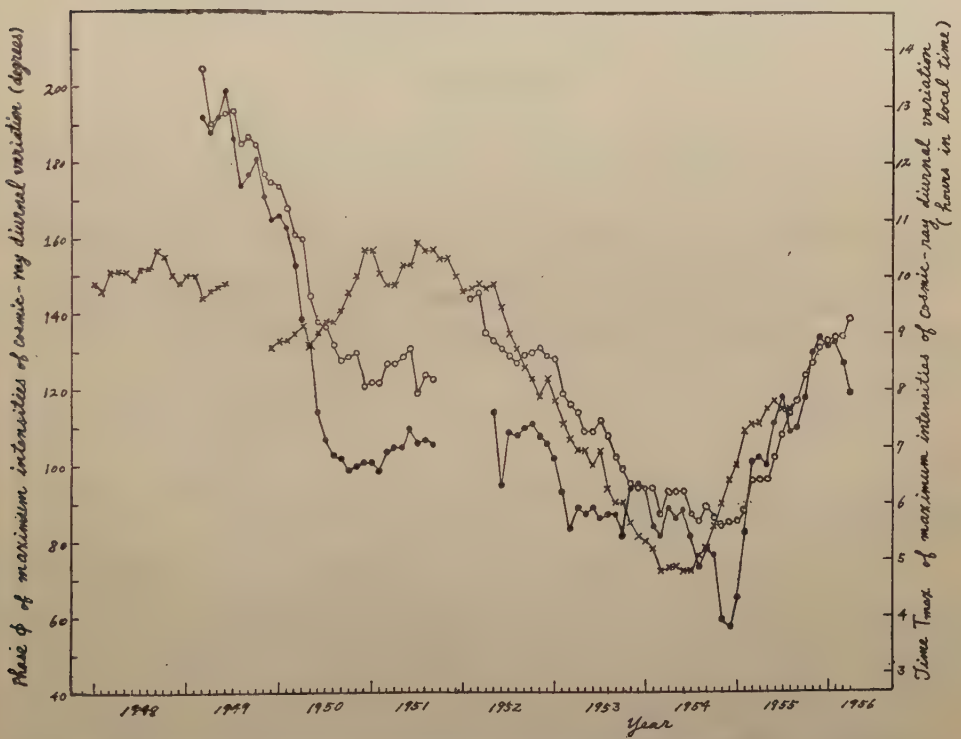

Fig. 12b The times of maximum intensities of 12 months' averages of 1st harmonics of cosmic-ray diurnal variations are plotted in every month.
●—●: T, ○—○: W, ×—×: $N3$

increase. That is, this increase of amplitude of cosmic-ray diurnal variation may be closely connected with the increase of K-index, not being rather associated with relative sunspot number.

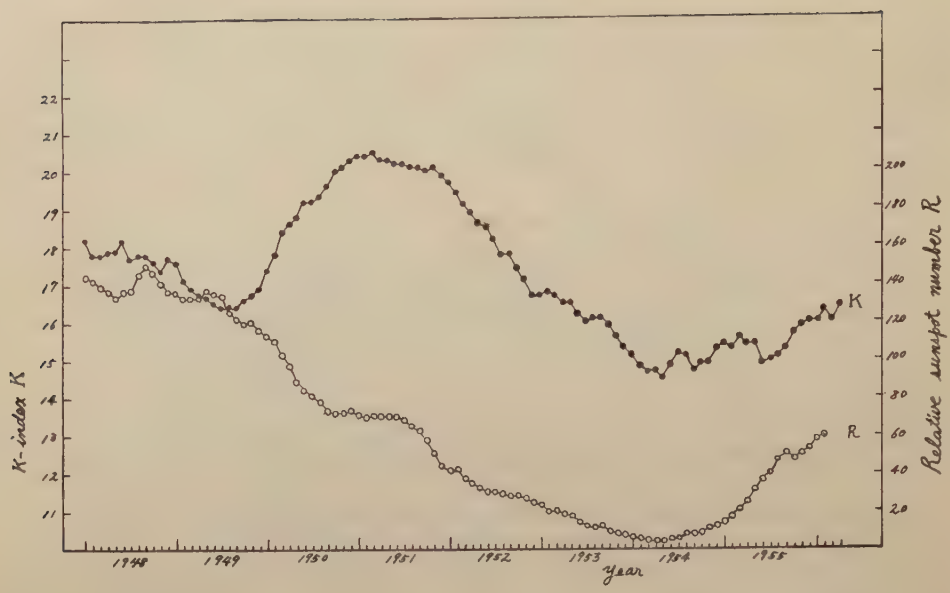

Fig. 13 12 months' averages of K-index K (monthly mean of daily sum) and that of relative sunspot number R (monthly mean) are plotted in every month.

7. Summary

1) Mean solar diurnal variations of cosmic-ray intensities of total component T and high energy component H penetrating 90 cm lead absorber measured with narrow angle telescope directed vertically show the phase difference of about 30 degrees from each others.

2) Though it is well known that anomalous solar diurnal variation S_D of cosmic rays appears at the time of geomagnetic storms, the existence of S_D about T and H were confirmed also.

3) Amplitude of S_D of T is the largest and about five times as large as those measured with wide angle telescopes.

4) The time of maximum intensities of S_D of H is the latest. The phase difference between T and H is about 60~90 degrees.

5) The phases of S_D are different with five different kinds of cosmic-ray meters in our country. The difference can be understood qualitatively by the difference of deflections of cosmic rays in the earth's magnetic field and the mean energies of cosmic rays measured with corresponding cosmic-ray meters.

6) The dispersion of the directions of S_D of individual geomagnetic storms measured with wide angle telescope is very large, but most of their directions are inside ± 90 degrees from the direction of their mean S_D.

7) S_D in every year measured with wide angle telescope point out about a definite direction, while quiet days diurnal variation shifts from year to year, corresponding to the known secular variation.

8) The amplitudes of mean solar diurnal variation of cosmic rays increase from

1952 and its increase is especially remarkable for T. It may be connected with the remarkable increase of K-index, not being rather asociated with relative sunspot number.

We intend to continue this experiment with narrow angle telescope directed vertically with higher accuracy and better stability than the present one.

8. Acknowledgement

The authors wish to express their cordial thanks to professor Y. Sekido for his guidance through many stimulous discussions and encouragement throughout this work. Mr. Miyazaki have generously allowed them to use the lead absorber for this research. The cosmic-ray data observed with wide angle telescope were supplied from Cosmic-Ray Laboratory of the Scientific Research Institute, Tokyo. The data of barometric pressure were supplied from Nagoya Distinct Meteorological Observatory, those of temperature of upper atmosphere from Central Meteorological Observatory, Tokyo, those of geomagnetism from Kakioka Geomagnetic Observatory, Kakioka and those of solar phenomena from Tokyo Astronomical Observatory, Tokyo. It is a pleasure to express their thanks to each of them. Thanks are also due to each members of Cosmic-Ray Laboratory, Nagoya University, for many critical discussions.

References

[1] Y. Sekido and S. Yoshida, Rep. Ionosphere Res. Japan, **4**, 37 (1950); D.W.N. Dolbear and H. Elliot, Journ. Atm. Terr. Phys. **1**, 215 (1951); Y. Sekido, S. Yoshida and K. Kamiya, Rep. Ionosphere Res. Japan, **6**, 195, (1952).

[2] Y. Sekido, M. Kodama and T. Yagi, Rep. Ionospere Res. Japan, **4**, 207 (1950).

[3] E. Brunberg, Recueil des Travaux de L'observatoire du Pic-Du-Midi, Serie (Rayons Cosmiques), 3 (1953).

[4] S. Yoshida, Geophysical and Cosmological Aspects of Cosmic Rays (Communications to the Meeting of I.U.P.A.P., at Guanajato, Mexico, in Sept. 1955, compiled by Work. Assoc. Prim. Cosm. Ray Res., Japan), 23 (1955).

[5] E. Brunberg, Tellus **v**, **2**, 135 (1953).

[6] K. Nagashima, J. Geomag. Geoelect. **V**, **4**, 141 (1953).

[7] T.H. Johnson, Rev. Mod. Phys. 10, 230 (1938); H.V. Neher and W.H. Pickering, Phys. Rev. **53**, 111 (1938).

[8] K. Nagashima, J. Geomag. Geoelect., **III**, **3-4**, 100 (1951).

[9] H.V. Neher, "Progress in Cosmic Ray Phys., edited by J.G. Wilson," Amsterdam, 300 (1952).

[10] T. Thambiyahpillai and H. Elliot, Nature **171**, 918 (1953).

The Measurement of Magnetic Hysteresis in Rocks and Minerals at High Temperatures

By E. R. DEUTSCH

Physics Department, Imperial College of Science and Technology, London, England.

(Received Oct. 1, 1956)

Abstract

An experimental method is described, designed chiefly to furnish data for a study of the direction, and stability with time, of thermoremanence in rocks. Specimens were heated to the Curie point in an evacuated electric furnace. Two pick-up coils were arranged close to the gap of a tuned a.c. electromagnet providing a maximum field H of 2400 oersteds. These were balanced to make their resultant e.m.f. zero in the presence of H alone, and proportional to dI/dt when a specimen of intensity of magnetization I was in the gap. This e.m.f. was applied to the vertical plates of a cathode ray oscilloscope. The potential drop over a small resistance in the electromagnet input was applied to the deflection coils, giving a measure of H. Computations based on the resulting pattern on the c.r.o. screen yield a loop of the I–H type, with I in arbitrary units, from which the coercivity can be evaluated. A pronounced "sawtooth" pattern has been observed in the (dI/dt)–H traces of pyrrhotite and franklinite specimens, particularly just below the respective Curie points.

The Continuous Recording of Hysteresis Curves

Several investigations [1], [2], [3], [4] have been made into the magnetic hysteresis of rocks, generally by stepwise measurements using a ballistic arrangement or a magnetometer. This method is slow and particularly unsuited to high temperature work when it is difficult to maintain experimental conditions constant for long periods.

Cathode rays were used, first by Ångström [5] and later by others [6], [7], [8], [9] for the investigation of the hysteresis curves of strongly ferromagnetic materials. Bruckshaw and Rao [10] first used an oscilloscope to measure the hysteresis of rocks. Air-cored coils, driven by a generator at 500 c/s, provided the field H. The e.m.f. across an assembly of balanced pick-up coils was zero in the absence of the specimen, and proportional to dI/dt when a specimen of intensity of magnetization I was introduced into one of the coils. This e.m.f. was applied to the vertical plates in the c.r.o. The potential drop across a small resistance in series with the input was applied to the horizontal plates, the resulting deflection providing a measure of H. A pattern of the (dI/dt)-H type was then traced on the c.r.o. screen. A numerical

integration of the vertical sweep was required to convert this into an *I–H* loop. Igneous rocks were investigated at room temperature in maximum fields of 750 oersteds.

Experimental Requirements

It can be shown that the field required to saturate spherical grains of magnetite falls in the range of 2000 to 3000 oersteds at room temperature. For several other strongly ferromagnetic minerals the saturation field appears to be also of this order. The equipment should therefore be designed to provide a magnetizing field of 2000 to 3000 oersteds. This field, as well as the temperature, must be as nearly possible constant over the volume occupied by a standard specimen, i.e. 4 to 5 cm^3 in the equipment described here.

The method must be capable of measuring the relatively small intensity of magnetization of a specimen, in the presence of the magnetizing field. For a standard specimen of incremental volume susceptibility 2000×10^{-6} c.g.s. units, measured in a weak field, this intensity accounted for roughly one part in 2000 of the total induction in the equipment employed.

To make observations up to the Curie points of the materials concerned, a maximum temperature of 600°C was necessary for the ferromagnetic minerals here examined, and this involved a satisfactory method of measuring the temperature. To prevent oxidation of the specimen in the laboratory, it must either be surrounded by an inert atmosphere, such as nitrogen or argon, or heated in a vacuum.

Summary of the Method

The method used by Bruckshaw and Rao, briefly described above, was modified for work at high temperatures. A tuned circuit at 50 c/s in which an electromagnet acted as the inductance now provided magnetizing fields up to 2400 oersteds. Two coils were placed near the air gap, the first being mounted on the core. The second coil, in an adjustable position outside the core, was threaded by part of the flux spreading outwards from the gap. These coils were balanced in such a way that the e.m.f.s set up in them by the magnetizing field alone, cancelled out.

The specimen was in a vacuum inside an electric furnace. With specimen and furnace in the gap, the alternating field magnetized the specimen, causing a negligible increase in the total flux of the magnetic circuit. Due to the respective positions of the pick-up coils in relation to the gap, a differential e.m.f. was produced, and was directly proportional to dI/dt of the specimen.

This e.m.f., after suitable amplification, was applied to the vertical deflection plates of an oscilloscope. The potential drop along a small resistance in series with the electromagnet was applied to the horizontal deflection coils of the oscilloscope, giving a measure of H.

Again it was necessary to convert the vertical scale from dI/dt to I, and these calculations were made on data obtained from an enlarged photograph of the

pattern, yielding a hysteresis loop of the *I–H* type, in which *I* was in arbitrary units.

The Magnetizing Field

Electromagnet (Fig. 1)

To avoid eddy currents, the core was built up from suitably trimmed transformer laminations of "stalloy," a high-permeability silicon steel. *A* 3cm gap was left between the pole pieces, which were interleaved with the yoke to prevent breaks in the magnetic circuit.

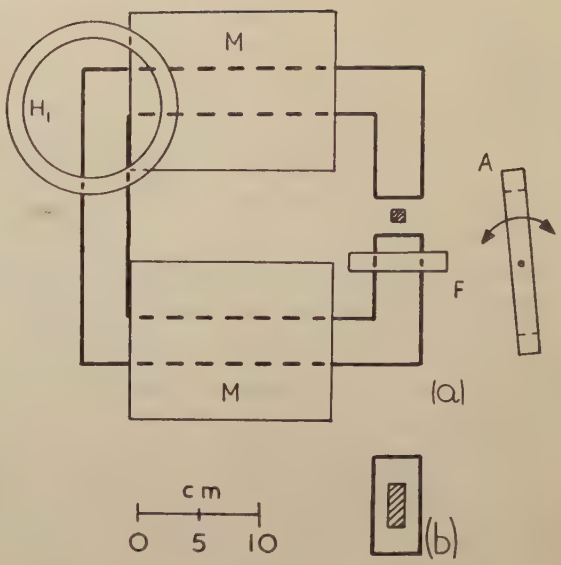

Fig. 1

Two magnetizing coils *M*, each of 1000 turns of no. 16 S.W.G. specially insulated copper wire, were wound on Tufnol formers of rectangular cross-section to fit the yoke in the position indicated in Fig. 1. The complete electromagnet was assembled with Tufnol clamps and bolted to a wooden table in a horizontal position.

Tuning Circuit (Fig. 2)

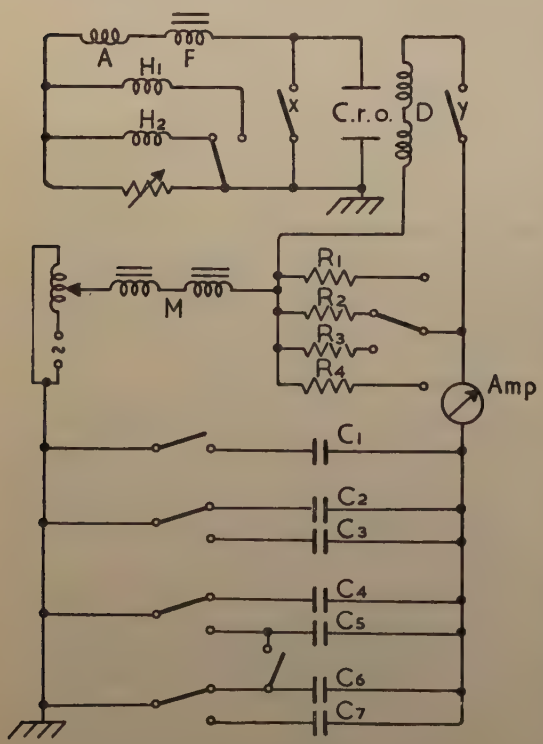

Fig. 2

The power for the magnetizing coils was obtained from the mains through an auto-transformer which supplied a maximum of 270 V, insufficient to drive more than a small fraction of the required current through the coils of total impedance 720 Ω. The impedance was reduced by a condenser *C* in series with the coils. Since the permeability of the core varied with the field, the self-inductance was a function of the magnetizing current, and a range of capacities was necessary to obtain different peak fields.

Since the gap was wide, the largest flux-density attained by the electromagnet was only 1700 *G*, at 3 amp (both r.m.s. values), corresponding to a field of amplitude 2400 oersteds. All fields up to this maximum could be obtained by tuning the magnetizing coils with the range of capacities 3.7

to 4·3 μF.

Measurement of the Magnetizing Field

A search coil whose effective area and shape were approximately those of a standard specimen could be positioned centrally in the gap. The reading on an a.c. voltmeter, multiplied by the appropriate factor, then gave the *average* field amplitude H_0 over the specimen volume.

A *gap survey*, carried out with a smaller search coil, revealed that the field in the volume occupied by a standard specimen varied by $\pm 2\%$ from this average, the maximum field being found along the line joining the centres of the pole pieces.

The Pick-up Circuit

A rectangular former F wound with 200 turns of no. 30 S.W.G. enamelled copper wire was fixed rigidly to one of the pole pieces, the coil centre being 3.7 cm from the gap centre.

The second, adjustable pick-up coil A, with 2500 circular turns of double silk-covered wire (40 S.W.G.) was placed close to the gap, to be threaded by some of the flux spreading outwards. As the ratio of the flux lines threading each of the two coils varied slightly for different magnetizing fields, the air-cored coil could be balanced by rotation with a fine adjustment control. Both formers and the adjusting mechanism were made of Tufnol.

Harmonics Coils

When the fundamental frequency was balanced a small e.m.f. remained, consisting at the lower fields chiefly of third harmonic. The relative positions of the two pick-up coils (Fig. 1) were chosen by trial to give a minimum of these harmonics.

A large coil $H1$ of 2100 turns was mounted in a position (Fig. 1) where the resultant flux due to the field surrounding the two magnetizing coils was zero at the fundamental frequency. The e.m.f. set up in this coil then consisted mainly of third harmonic. After suitable adjustment of the amplitude by a potentiometer in the circuit, this was balanced against the harmonic residue in the pick-up coils, most of which was eliminated by this method. In fields above 1500 oersteds, a small coil $H2$ of 900 turns (Fig. 2) reduced the amplitude of the undesirable harmonics, but since these were now more complex, they balanced only to a minor degree. Both harmonics coils were made of double silk-covered copper wire (40 S.W.G.) wound on Tufnol formers whose position above the electromagnet was adjustable.

All the leads of the pick-up circuit (Fig. 2) were electrostatically screened.

The Oscilloscope Pattern

The oscilloscope was a Cossor double beam instrument giving a blue screen pattern.

Vertical Deflection.

The output of the pick-up system was fed into the c.r.o. amplifier, with a maximum gain of 900, and the amplified e.m.f. applied to the vertical plates of the

tube.

Horizontal Deflection.

The potential drop across a small resistance R in series with the electromagnet was applied to the c.r.o. deflection coils D. The plates could not be used since both pairs, as well as the autotransformer, were earthed on one side. Depending on the input current, the tapping was made from one of a set of nichrome resistances in the range 0.3 to 1.7 Ω, selected to give full screen deflection.

By means of suitable switches x and y in the c.r.o. input, the coordinate axes could be superimposed on the photograph of each pattern.

Deflection Calibration.

The deflections on the tube screen were found to be proportional to the input, up to the dimensions of the pattern. These were generally confined within a central area of 5 cm diameter, where the screen was made flat to eliminate curvature error.

Photography

A Cossor 35 mm camera with manually operated shutter was used. Blue-sensitive Kodak *R*20 and Ilford 5 Bll films were selected, both types having high resolution. With low brilliance to render fine outlines on the curves, a suitable exposure for patterns was $\frac{3}{4}$ s. The axes required much shorter timing.

Furnace and Thermocouples

The *furnace* (Fig. 3), essentially a long quartz tube wound with resistance wire, was of the general type used by Tomlinson and Bockris [11] in the range 1000 to 2000°C. It was sufficiently narrow to fit between the pole pieces, leaving an air cushion 2 to 3 mm wide on each side.

A short, perforated quartz tube, fused inside to the bottom of the furnace, supported a quartz crucible containing the specimen. Heat conduction away from the crucible was thus greatly reduced, whilst convection was overcome by evacuating the tube through an outlet. A ground pyrex cone sealed the furnace vacuum-tight at one end, and, since the vacuum grease melted after slight heating, the furnace top was water cooled. Tungsten rods sealed through the pyrex provided contacts for the thermocouple.

The furnace was wound with 43 turns of no. 27 S.W.G. "nonmagnetic"

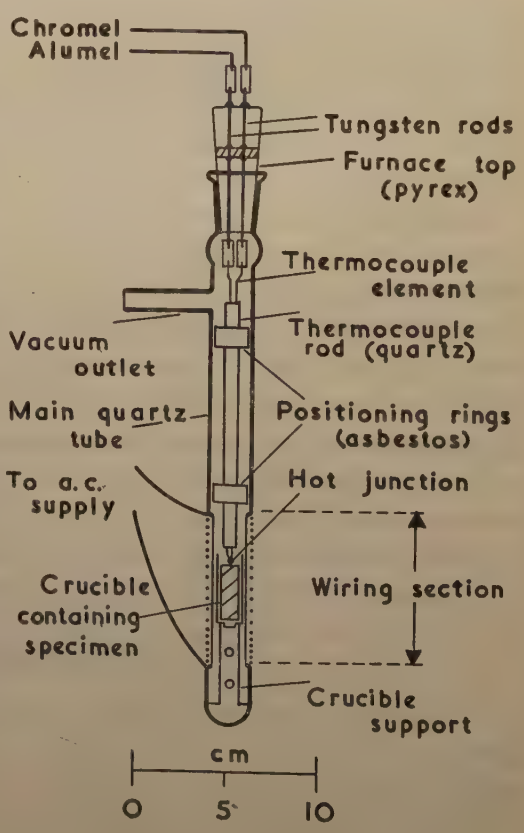

Fig. 3

nichrome wire, concentrated at the top and bottom. With this arrangement, the temperature in the region normally occupied by a specimen was found to vary by ±1% from its average value. A sheet of mica surrounding the wiring section, together with the air cushion, provided partial heat insulation for the pole pieces. Since, at high temperatures, the tube was left in the gap for at most 15 s., further insulation was found unnecessary. The a.c. supply from an auto-transformer heated a specimen to 600°C in 10 min, with 2.75 amp, but no advantage was gained from heating so quickly. To prevent induction in the pick-up coils from the heating coil, the supply was cut off for a short interval during the photographic exposure. During this interval the specimen temperature dropped by about 1°C at 600°C, and this was neglected.

The furnace was kept in a raised position until the required temperature was reached, and then lowered into the gap by means of a brass ratchet arrangement.

Thermocouple Circuit

A chromel-alumel element yielding a large thermal e.m.f. was used. The junction was arc-welded into a bead, in a reducing atmosphere. To diminish the magnetic effect caused below 140°C by the nickel in chromel and alumel, the thermocouples were made of no. 26 S.W.G. wire, the smallest gauge available at the time. Any remaining magnetic background was accounted for by subtraction of the oscillogram pattern due to the thermocouple alone, from that obtained jointly with specimen and thermocouple. This precaution was only necessary with a few relatively weakly magnetic specimens. The hot junction was positioned centrally inside the furnace (Fig. 3).

A chromel-alumel cold junction was placed in ice inside a Dewar flask. Readings were taken on a galvanometer whose full deflection corresponded to about 60°C, the higher temperature ranges being obtained by using suitable resistances in the circuit. To prevent secondary thermal e.m.f.s., all the wire in the thermocouple circuit was thick chromel or alumel. Pairs of metal contacts at the galvanometer, furnace top, cold junction head and switches, respectively, were closely spaced to equalize the temperature of each pair.

Accuracy of Temperature Measurements

A standard platinum-platinum/rhodium couple was used to calibrate two chromel-alumel elements. The latter gave readings differing by up to 2°C at 600°C, where the temperature could be read to 1°C. Together with smaller errors, due to local heating at contacts, lag in the galvanometer response, etc., the uncertainty in the temperature determination may have amounted to ±5°C at 600°C.

The Vacuum System

The furnace was evacuated by means of a two-stage pump, the vacuum circuit being thick-walled rubber tubing sealed to glass connections with wax. The vacuum, measured with a mercury level gauge, averaged about 1 mm of mercury, sufficient to prevent any significant oxidation of specimen or thermocouple in the temperature range used.

The Specimens

Specimens investigated included the strongly ferromagnetic minerals magnetite, pyrrhotite and franklinite, as well as rocks such as basalts, in which magnetite or titanomagnetite commonly occur as minor constituents. Specimens were cut into prisms 3.0 cm long and 1.1×1.1 cm in cross-section. When powder concentrations of a ferromagnetic mineral were required for study, the mineral powder was mixed with plaster of Paris powder. Water was added and the resulting paste allowed to set in a mould. Artificial "rock" specimens were thus produced.

Computation of the Hysteresis Curves

If H denotes the field in the magnetic circuit and B the induction, then $H=B$ in the air gap. A specimen sets up further lines of induction, such that

$$B=H+4\pi I \qquad (1)$$

where I is its intensity of magnetization. Since B, H and I are vectors, this relation is numerically exact only for specimens saturated in a uniform field. Using an a.c. electromagnet, the e.m.f. set up in a pick-up coil is then proportional to dB/dt, where

$$dB/dt=dH/dt+4\pi(dI/dt). \qquad (2)$$

Since dH/dt is balanced out in the method used, the field term vanishes and the net e.m.f. becomes proportional to dI/dt only. For a sinusoidal input current of frequency f

$$H=H_0 \sin \omega t \qquad (3)$$

where H_0 is the peak field and $\omega=2\pi f$.
So

$$dH/dt=H_0\omega \cos \omega t, \qquad (4)$$

and since

$$dI/dt=(dI/dH)\times(dH/dt) \qquad (5)$$

$$dI/dt \propto (dI/dH)\cos \omega t. \qquad (6)$$

An ideal pattern on the c.r.o. screen is then proportional to expression (3) horizontally and to (6) vertically. In practice, the length of the horizontal trace increased linearly with H up to nearly 1200 oersteds, but at higher fields this increase became larger as H was raised, and it was necessary to calibrate the x-axis.

A calibration chart contained the coordinate axes as well as vertical lines intersecting the abscissa at intervals corresponding to steps of $0.05 H_0$. This was accurately superimposed on a projected oscillogram of the pattern, whose height could then be measured directly at regular field intervals. A typical

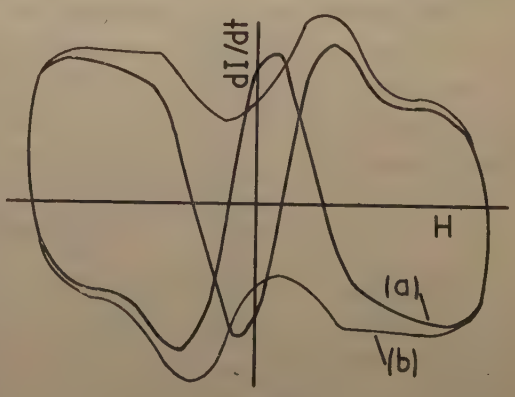

Fig. 4

oscillogram, taken at $H_0=2300$ oersteds, has been retraced in Fig. 4. At each interval, the difference between the main loop (a) and loop corresponding to unbalanced harmonics (b) was measured, giving net readings caused by the specimen alone. Values proportional to dI/dt thus obtained along the ordinate were converted into quantities proportional to dI/dH after division by $\cos\omega t$ (Fig. 5). A numerical integration between limits of $0.05H_0$, proceeding from the origin at an arbitrary abscissa, then yielded the desired I–H curve (Fig. 6a).

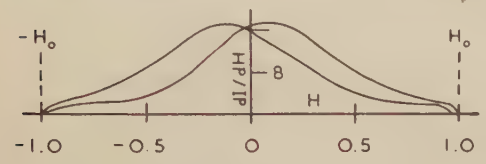

Fig. 5

Half the vertical separation between the maximum and minimum of I was taken as the *saturation magnetization* I_s. Half the separation between the intercepts at $H=0$ gave the *remanence* I_r. The horizontal axis could be obtained by locating a point along the ordinate axis either halfway between $+I_s$ and $-I_s$, or halfway between $+I_r$ and $-I_r$. In an ideal hysteresis loop these points should coincide at the true origin, but due to experimental errors involving mainly the oscilloscope measurements, the loop may be slightly distorted and fail to close. When this has been the case (Fig. 6b), the final abscissa was drawn through an origin located in a mean position along the ordinate. Half the separation between the intercepts on the abscissa then yielded the *coercivity* H_c.

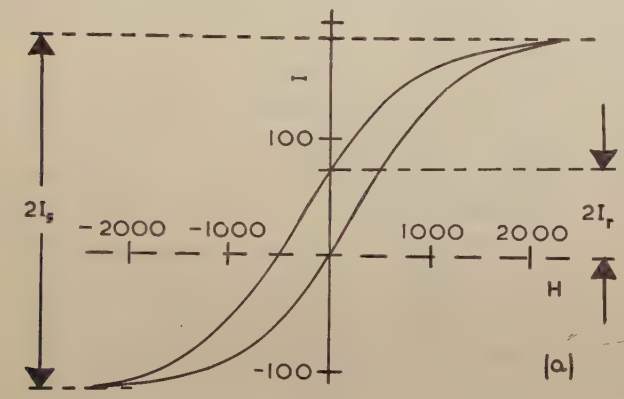

Fig. 6a

From the distortion in the quoted example, H_c, I_r and I_s were estimated to be accurate to ± 1.6, 2.5 and 0.6% respectively. These may be regarded as typical figures for strongly magnetic rocks. In smaller fields, involving simpler patterns, these errors decrease, whilst measurements at high temperatures or with weaker rocks entail correspondingly larger errors. Just below the Curie point, the I–H loop tends to become very flat, and then the expected error in measuring H_c may be as large as 10 to 20%.

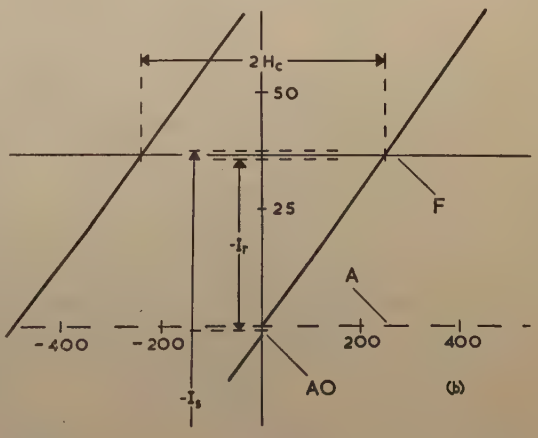

Fig. 6b

The "Sawtooth" Pattern

In Fig. 7 (a—f), oscillograms are reproduced for a pyrrhotite specimen ($P1$) at $H_0=1200$ oersteds and temperatures between 20°C and 310°C. To

facilitate the computing, the harmonics loop was expanded to surround the main pattern, which remained relatively unchanged up to 210°C, but rapidly altered between 295°C and 310°C, corresponding to the collapse of the *I–H* loop just below the Curie point.

At high temperatures, the oscillograms exhibited the "sawtooth" pattern (Fig. 7 (c—f)), which was most pronounced in the region of the coercive field and affected those parts of the loop where magnetization changes are likely to proceed chiefly through irreversible domain movements. The pattern resembled a damped oscillation with a regular period.

A phenomenon possibly analogous to this has been observed by Cross [12] in the neighbourhood of the electrical coercive field of barium titanate crystals, where a "kinking" occurred at a certain temperature below the Curie point. In the present case, however, the "sawtooth" pattern was not noticeable in the computed *I–H* loops, except when they were greatly enlarged.

Three other examples of the "sawtooth" pattern, retraced in Fig. 8 (a—c), appeared to be most pronounced in the range 15°C to 50°C below the Curie points concerned (Table I).

Results of hysteresis measurements on a number of specimens are discussed in a separate paper in this issue of the Journal.

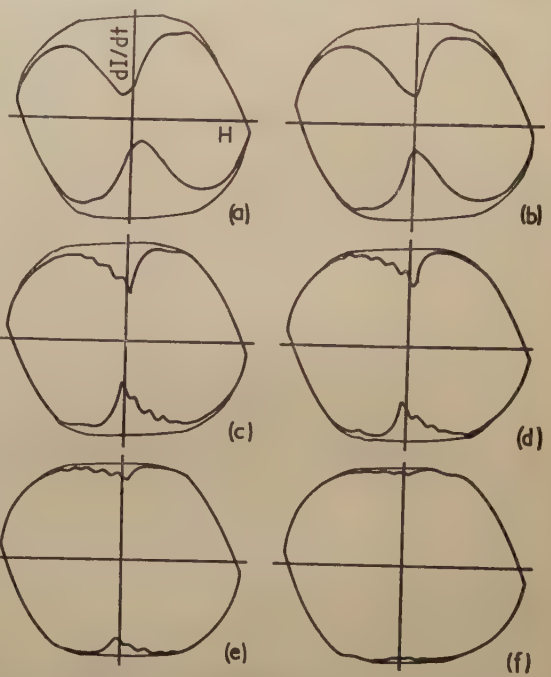

Fig. 7

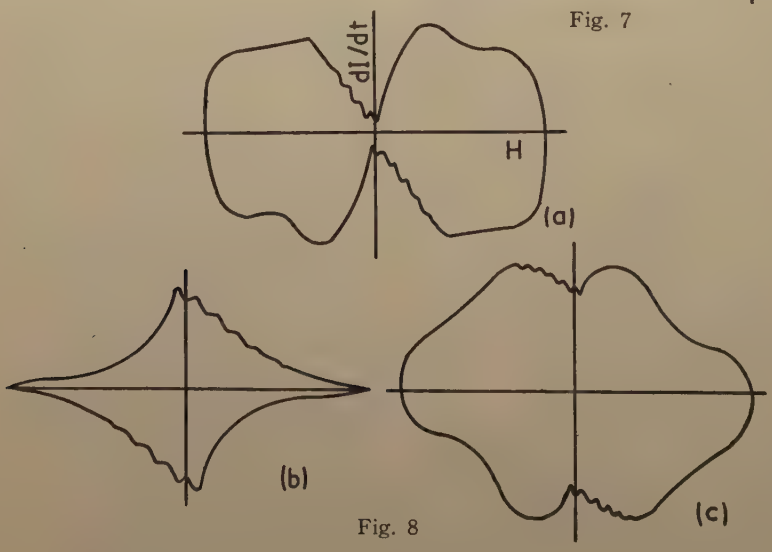

Fig. 8

Table I. *Temperature of pronounced "Sawtooth" patterns*

Specimen	T_c (°C)	T_s (°C)	T_c–T_s (°C)
*P*1 (Pyrrhotite)	330	305-300	25–30
*P*2 (Pyrrhotite)	320	295–270	25–50
*F*4 (Franklinite)	20	5	15
*F*5 (Franklinite)	525	480	45

T_c=Curie point.
T_s=Temperature(s) at which pattern was photographed.

Acknowledgments

The author wishes to express his gratitude to Prof. J.M. Bruckshaw, *F.* Inst. *P.*, for his help and encouragement throughout the work. Thanks are also due to the Anglo-Iranian Oil Company and the Anglo-Saxon Oil Company for providing the financial basis for this research.

References

[1] Nagata, T. Rock Magnetism, p. 105 (Tokyo: Maruzen and Co., Ltd., 1953).
[2] Puzicha, K. Z. Prakt. Geol. **38**, 161, 184 (1930).
[3] Turcev, A. Bull. Acad. Sci. U.S.S.R. (Leningrad), Ser. 7, Phys.-Math. Sci., 89 (1928).
[4] Tzu-Chang-Wang. Z. Geophys. **16**, 160 (1940).
[5] Ångström, K. Phys. Z. **1**, 121 (1899); Phys. Rev. **10**, 74 (1900).
[6] Cosens, C.R. Wireless Engr. **12**, 190 (1935).
[7] Johnson, J.B. Bell Syst. Tech. J. 8, 286 (1929).
[8] Kreiselsheimer, K. J. Sci. Instrum. **19**, 137 (1942).
[9] Madelung, E. Phys. Z. 8, 72 (1907).
[10] Bruckshaw, J.M. and Rao, B.S. Proc. Phys. Soc. (London) **63**, 931 (1950).
[11] Tomlinson, J.W. and Bockris, J. O'M. Rev. Sci. Instrum. **21**, 507 (1950).
[12] Cross, L.E. Phil. Mag. **44**, 1161 (1953).

The Magnetic Hysteresis of Rocks and Minerals at High Temperatures

By E. R. DEUTSCH

Physics Department, Imperial College of Science and Technology, London, England.

(Received Oct. 1, 1956)

Abstract

The coercivity, remanence and saturation magnetization of a number of minerals and rocks have been obtained as a function of temperature, using alternating fields up to 2300 oersteds. These results suggest that most of the specimens examined can retain thermoremanence for long periods, even at high temperatures. Irregularities occurring in some of the temperature curves indicated the presence of more than one ferromagnetic constituent. Heat treatment in several cases caused considerable changes in the hysteresis curves measured at atmospheric temperatures. The thermomagnetic behaviour of two basalts has supported the view that the reversed magnetization of certain rock formations is due, not to abnormal magnetic properties on the part of the material concerned, but to a past reversal of the geomagnetic field.

Introduction

As a result of field and laboratory work undertaken since 1946 by the Geophysics Department of the Imperial College, it has been discovered that the Tertiary tholeiite dyke system of Northern England is permanently magnetized in a direction opposite that of the present earth's field [1]. It was subsequently shown [2], [3] that many of the Tertiary lava flows and dykes of the Isle of Mull possess statistically significant mean directions of magnetization, some of which are in opposition to the geomagnetic field, whilst others nearly coincide with it. Reversals in the polarization of igneous rock formations have been discovered in many countries, including South Africa, Iceland, Japan, France, etc.

Igneous rocks usually acquired their natural residual magnetism while cooling in the earth's magnetic field from temperatures above their Curie points. This "thermoremanence" may exceed by a large factor the magnetization induced in the rock by the present geomagnetic field at atmospheric temperatures. Laboratory experiments carried out on the Mull rocks showed that nearly all the significantly polarized specimens exhibited thermoremanence. When cooled from above their Curie points, they always became magnetized in the direction of the acting field. To explain the occurrence of reversed magnetism in the rock formations concerned, it was postulated that the geomagnetic field itself was reversed at the time when they originally cooled through the Curie points of their ferromagnetic constituents.

As an alternative to this hypothesis, Néel [4] and others have suggested that an intrinsic property of the rocks themselves may account for their reversed polarization. In support of this, a number of Japanese specimens do acquire thermoremanence in the laboratory, in opposition to a small applied field [5], [6]. An ultimate decision in favour of one or the other of the two basic theories thus requires further research into the magnetic and thermomagnetic properties of rocks.

In a paper by Bruckshaw and Rao, [7] experiments are described in which the magnetic hysteresis of rock specimens, mainly from the tholeiite dykes, was measured in fields of 750 *Oe*. Large coercivities were obtained, comparable to those of certain magnet steels. These data permitted the assumption, essential to the field reversal hypothesis, that the inversely magnetized Tertiary rocks have retained a large proportion of their original polarization for 30 million years, perhaps mainly in opposition to the earth's field.

The present paper deals with the results of an extension of the above work into a study of the magnetic hysteresis of minerals and rocks at temperatures up to their Curie points. The experimental method used is the subject of a separate paper in this issue of the Journal. The knowledge thus gained can allow deductions to be made about the stability of thermoremanence. For example, the coercivity of a basalt with its Curie point at 580°C may exceed −100 oersteds in the entire range from 500°C to atmospheric temperature. It is then safe to conclude that the rock will be capable of retaining the direction of its original thermoremanence not only for long periods and in opposition to the ambient field, but even if partial reheating should subsequently occur. Very few data on this subject have been published. Koenigsberger [8] measured the coercivity of a hematite specimen up to 500°C and found that it decreased rapidly at first, but more gradually at the higher temperatures. Akimoto [9] reported a similar behaviour for the case of the ferromagnetic constituents separated from an andesite sample, while Forrer [10] observed that the coercivity of a magnetite crystal decreased steadily up to its Curie point.

Results

If the specimens were saturated at room temperature in a field of 2300 *Oe.*, the usual terms *coercivity* (H_c), *remanence* (I_r) and *saturation magnetization* (I_s) will be used. If saturation was not achieved at 20°C, the corresponding terms *coercive force* (H_c'), *residual magnetization* (I_r') and *maximum magnetization* (I_s') will be used at *all* temperatures.

The rock and mineral samples were cut into rectangular prisms of approximate 1.2 cm^2 section by 3.0 cm length, the field being applied perpendicular to the long axis. Magnetite, pyrrhotite, franklinite and one rock type, basalt, were investigated. Except for one powdered magnetite, all specimens were cut from natural rock samples.

(1) *Magnetite*

(a) Magnetite from Pretoria, South Africa, (specimen *M*1) was observed at 20°C and then at a sequence of temperatures as the rock cooled from 604°C. The maximum

field H_0 was 2300 *Oe.* in all cases.

The results (Fig. 1) show the Curie point of the specimen in the range 580–585°C, in good agreement with the value for pure magnetite. The saturation magnetization shows its sharpest drop between 400 and 435°C. On the basis of the domain theory, I_s represents the sum of the spontaneous magnetizations of all the domains in a material and, for pure magnetite, the curve of I_s against T should be smooth, I_s falling more and more rapidly as the Curie point is approached. Specimen $M1$ therefore is likely to contain a second constituent with its Curie point in the neighbourhood of 435°C, possibly a titanomagnetite, which is the name generally given to a magnetite containing $TiFe_2O_4$ (ulvöspinel) in solid solution. Since ulvöspinel is paramagnetic, its concentration in the solid solution determines the magnetic properties, including the Curie point, of the titanomagnetite.

The temperature curves were all irreversible (Fig. 1), the value of I_s at the end of the experiment being only 17% of that determined before the specimen had been heated. Akimoto [11], [12] also obtained irreversible I_s–T curves. These results suggest that specimen $M1$ initially contained maghemite (γ-ferric oxide) which turned into the α-form (hematite) after heating. Due to defects in its crystal lattice, maghemite can be strongly ferrimagnetic, but it becomes unstable when heated and turns into hematite at 275°C, according to some observers, and at 400–800°C, according to others. The Curie point of both ferric oxides is given as 675°C. Hematite is possibly ferromagnetic, with low values of I_s and I_r but high values of H_c, possibly several thousand oersteds [13]. This would account for the uncommonly large coercivity (−613 *Oe.*) exhibited by the specimen at 20°C after heating. Koenigsberger [14] also examined magnetite from Pretoria and found $H_c = -380$ *Oe.* for a solid sample and $H_c = -450$ to -570 *Oe.* for a powder. On the other hand, he observed that "titanomaghemites" yielded principally magnetite rather than hematite after prolonged heating to 700°C. The fact that no Curie point above 585°C was observed in specimen $M1$ suggests magnetite as the end product, but since α-ferric oxide is only very weakly magnetic, especially at high temperatures, its presence may have remained undetected. A final decision must await chemical or X-ray analysis of the material.

(b) Specimen $M2$ was cut from the same original sample of Pretoria magnetite as $M1$, and H_c, I_r and I_s were measured at room temperature before heat treatment,

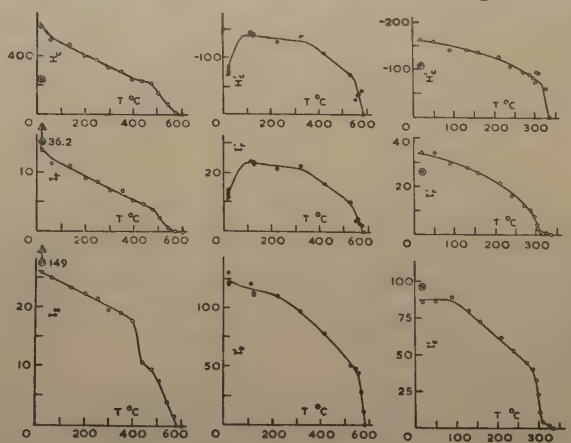

Fig. 1 Specimen $M1$. Magnetite

Fig. 2 Specimen $M3$. Magnetite

Fig. 3 Specimen $P1$. Pyrrhotite

Points obtained ⦿ before heating; ● whilst heating; ○ whilst cooling.

H_c and H_c' in oersteds; I_r, I_r', I_s and I_s' in arbitrary units.

and after heating to 600°C on four successive occasions. By far the greatest changes resulted from the *first* heat treatment (Table I), and these were of the same order of magnitude as in specimen *M*1.

Table I. *Specimen M2—changes due to heat treatment*
$T=20°C$. $N=$*Number of times the specimen has been heated to* 600°C.

	oersteds	arbitrary units	
N	H_c	I_r	I_s
0	−273	46.0	153.1
1	−591	16.3	31.1
2	−672	8.2	10.6
3	−682	7.9	9.3
4	−607	8.0	14.0

(c) As several observers have pointed out, [15] the magnetic properties of rocks can be reduced essentially to those of the ferromagnetic minerals contained in them. Magnetite from Tintagel (Cornwall) was powdered and the magnetic constituent extracted with a magnet. Sufficient of the ungraded powder was added to plaster of Paris to produce an artificial specimen containing about 25% by weight of magnetite. Measurements were made at temperatures rising from 20 to 600°C, with $H_0=2300\,Oe$.

The Curie point was again in the neighbourhood of 585°C (Fig. 2), but the I_s'–T curve here resembles the I_s–T curves of a pure ferromagnetic material. The H_c'–T and I_r'–T curves exhibit a peculiar feature, both showing a rapid rise up to about 100°C. This effect may well be due to incomplete saturation at normal temperature. The location and magnitude of the resulting maximum would then depend on the manner in which I_s', I_r' and H_c' vary with field and temperature, respectively.

(2) *Pyrrhotite*

(a) Specimen *P*1, of undetermined origin, was examined upon cooling from 345°C in a field $H_0=1200\,Oe$. With increasing T (Fig. 3), the decrease of H_c' is more gradual than that of either I_r' or I_s', but all three curves fall to zero at 333°C. The sharpest drop in I_r' and I_s' occurs near 300°C, so that the region between 300 and 333°C possibly includes two Curie points. The *I*–*H* loops in Fig. 4 (a—d) show the rapid increase of hysteresis for a small temperature drop just below 333°C.

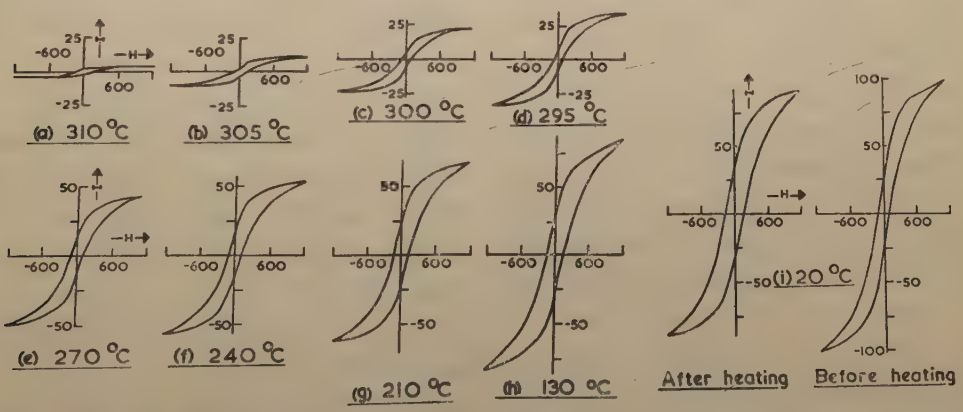

Fig. 4 Specimen *P*1. Pyrrhotite. *I*–*H* Curves.

At 20°C the hysteresis loop showed an approach to saturation. Several studies [16] have revealed the strong anisotropy of pyrrhotite crystals, which in certain cases

attain saturation only in very high fields. Davis [17] investigated powdered pyrrhotite which was not saturated at 3340 *Oe*. On the other hand, the hysteresis loop of a pyrrhotite specimen obtained by Tzu-Chang-Wang [18] shows near-saturation at 501 *Oe*., H_c being of the same order as in specimen *P*1.

(b) Specimen *P*2, from Sudbury (Ontario), retained ferromagnetic properties beyond the Curie point of pure pyrrhotite and was examined as it cooled from 590°C in a field $H_0=2300$ *Oe*. (Fig. 5). The I_s'–T curve terminates at 560–580°C, which is near the Curie point of magnetite. Its shape suggests that this curve contains two "simple" components of magnetite and pyrrhotite, respectively. Below the Curie point of pyrrhotite the curve is thus a resultant of the I_s'–T or I_s–T curves of each of these constituents, whilst above that temperature it represents magnetite alone. From the intersection of tangents drawn to the I_s'–T curve, the Curie point of the pyrrhotite was estimated to be 320–325°C. The irregular trend of H_c' near 300°C may have arisen as follows:—

At room temperature, the measured value of H_c' is intermediate between the separate coercive forces of pyrrhotite and magnetite. A comparison of Figs. 2 and 3 suggests that, in the neighbourhood of 300°C, H_c' of the magnetite is larger than that of the pyrrhotite, but that they both decrease with rising temperature. However, the contribution of the pyrrhotite to the total magnetization also diminishes until, at its Curie point, the value of the resultant coercive force is a maximum and represents magnetite alone. It follows that a minimum exists below this temperature, as confirmed in Fig. 5. A similar mechanism may account for the observed irregularity in the I_r'–T curve.

(3) *Franklinite*

All franklinite specimens have come from the Franklin (New Jersey) area, and *F*1 to *F*4 have been cut from a single sample.

(a) Specimen *F*1 was investigated as it cooled from 605°C in a field $H_0=1200$ *Oe*. The graphs in Fig. 6 suggest a Curie point just above 600°C. The H_c' maximum may be due to a mechanism similar to that responsible for the H_c' maximum of *M*3; this now occurred at 560°C, probably because saturation was not attained below that temperature. Towards room temperature, the trends of the I_s'–T and I_r'–T curves become concave upwards, instead of downwards as expected, the greatest changes occurring in the narrow range

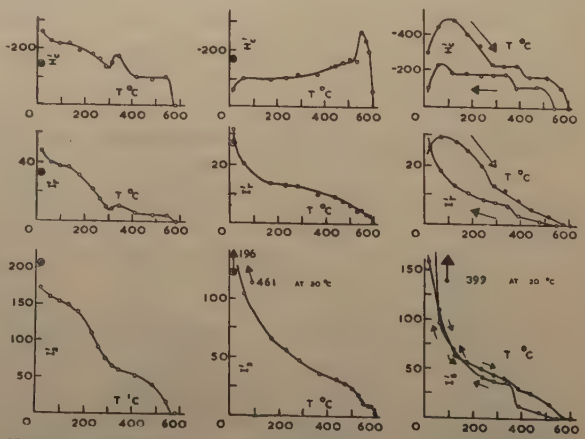

Fig. 5. Specimen *P*2. Pyrrhotite

Fig. 6 Specimen *F*1. Franklinite

Fig. 7 Specimen *F*2. Franklinite

Points obtained ◉ before heating; →● whilst heating; ←○ whilst cooling.

H_c' in oersteds; I_r' and I_s' in arbitrary units.

between 61 and 20°C, where I_s' increased by a factor of 4.4 and H_c' dropped sharply. Since ten hours had elapsed between the measurements at 61 and 20°C, respectively, it was considered possible that these marked changes in magnetic properties might depend on time.

(b) Specimen $F2$ was investigated during the heating as well as the cooling process. The field was increased to 2300 *Oe*, sufficient to cause saturation not far above room temperature; hence the location of both coercive force maxima at relatively low temperatures, (Fig. 7). Upon cooling from 610°C, the Curie point was lowered by about 60°C. Ten hours again elapsed before the final measurement was made, and the changes occurring between 62 and 20°C were of the same order of magnitude as those observed for $F1$ in the corresponding temperature range.

(c) To determine the time interval during which the large increases in magnetization occurred the experiment was repeated with a third specimen, $F3$. Again this was heated above 600°C. After cooling to 50°C, it was taken out of the furnace and transferred to an apparatus where volume susceptibility k was measured in a small field, at repeated intervals.

Table II. *Specimen F3—Volume susceptibility*
t=time in minutes since first reading was taken.
k=incremental volume susceptibility in c.g.s. units $\times 10^{-6}$.

t	k	t	k	t	k
—*	4,700	7.5	19,170	15.0	21,270
0	9,630	8.5	19,680	16.0	21,460
4.0	15,210	10.5	20,850	17.0	21,590
6.0	17,600	13.5	21,170	19.0	21,600

* Reading taken before the specimen was heated.

Table II shows that k increased steadily for the first 10 minutes and then approached a stable value. The reading at $t=19$ minutes should correspond to a temperature of 20°C and at $t=0$ the temperature should be in the range 30–40°C. In the time elapsed k had increased by a factor of 2.2, which is of the same order as the increases in I_s' for $F1$ and $F2$, in roughly the same temperature interval. The conclusion appears warranted that temperature rather than time effects were responsible for the peculiar magnetization changes observed in specimens $F1$–$F3$. It may be suggested that the first heating caused chemical alterations in the material, resulting in the formation of a new constituent having its Curie point near room temperature, or slightly above.

(d) To investigate the possibility of chemical action, a further specimen, $F4$, was subjected to the same heat treatment as $F1$–$F3$ and then cooled to −50°C by means of solid carbon dioxide. Inspection of Fig. 8, which shows the curves obtained in a field of 1200 *Oe.*, combined with those previously obtained for $F1$, but adjusted to the new scale, reveals an intensely magnetic constituent with a definite Curie point

in the low temperature range. Independent estimates from the I_r'–T and I_s'–T curves gave 15°C and 22°C, respectively. This compares with the value of 61°C, quoted by Wologdine, [19] the only reference to the Curie point of franklinite discovered in the literature. The coercive force minimum near 20°C is perhaps due to the interaction of the two constituents. A similar experiment with a specimen from the original franklinite sample, but which had not been heated, failed to disclose a low-temperature constituent of major intensity. The phenomena observed can thus be satisfactorily explained on the basis of chemical action caused by the heat treatment.

G.D. Nicholls, of the Department of Geology, University of Manchester, has examined some of the above specimens in powder form. He found that the original "franklinite" sample was really a mixture of

1. An opaque magnetic constituent, probably franklinite;
2. A green mineral, believed to be a pyroxene, or possibly willemite (zinc silicate);
3. A reddish brown mineral, perhaps tephroite (manganese silicate).

After heat treatment, mainly the opaque mineral, but also some of the silicate remained, thus confirming that chemical change had taken place. An X-ray powder photograph showed the cell dimensions of the opaque mineral to be very similar to those of magnetite, as would be expected in franklinite, but no detailed measurements were possible in this case.

It may be plausibly suggested that the chemical changes caused by heating resulted in a transfer of some Zn and Mn into the crystal lattice of the franklinite, which is a mixed ferrite, containing variable proportions of these atoms in its natural state already. It has been shown [20] that the addition to a ferromagnetic ferrite of zinc ferrite, which is paramagnetic at normal temperatures, produces mixed crystals whose Curie point is below that of the ferromagnetic ferrite. If manganese ferrite, whose Curie point is at 510°C, is also added, the magnetic properties of the ferromagnetic ferrite, in this case franklinite, are probably further modified. A mechanism on these lines may account for the phenomena observed with specimens $F1$–$F4$.

(e) The investigation was extended to specimen $F5$, cut from an entirely new sample of franklinite, which was measured at $H_0 = 2300\,Oe.$ upon cooling from 548 to 20°C, and at 0°C. At the lower temperatures, the trend in the I_r'–T and I_s'–T curves is again concave upwards, indicating once more a second constituent, though this appears to occur now in relatively small proportions.

Upon extrapolating these curves, a Curie point of 527°C was obtained. Part of the sample from which specimen $F5$ had been cut was examined by Nicholls and found to be a much purer "franklinite" than the previous specimens. This would suggest that the Curie point here observed is more representative of franklinite than that near 600°C, as in the case of $F1$ and $F2$, or near 20°C, as in the case of $F4$. Since the composition of even a "pure" franklinite is not rigidly defined, however, it may be meaningless to assign this mineral a definite Curie point, unless such a temperature is quoted in relation to the chemical composition of the specimen

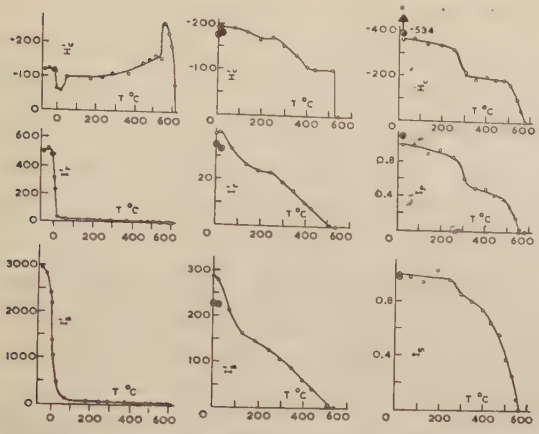

Fig. 8 Specimens *F*4 and *F*1. Franklinite

Fig. 9 Specimen *F*5. Franklinite

Fig. 10 Specimen *N*. "Normal" Basalt.

Points obtained ◉ before heating; ● whilst heating; ○ whilst cooling.

H_c and H_c' in oersteds; I_r, I_r' I_s and I_s' in arbitrary units.

concerned.

A more precise explanation of the phenomena here observed with franklinite would require a good deal of further work, including a detailed study of the chemical processes occurring during heat treatment.

(4) *Basalt*

Basalts commonly contain magnetite or titanomagnetite as minor constituents, in which case they exhibit ferromagnetic properties. In his work on the dykes and lava flows of Mull, Vincenz [2], [3] measured the directions of magnetization of a number of oriented samples from each rock formation he investigated, and computed a mean direction for that formation. The significance of this mean was assessed by a statistical analysis.

The experiments described below have been conducted principally to compare the temperature curves of rocks whose natural thermoremanence had been respectively normal and inverse in direction. To be fully representative of these two types of behaviour, the specimens were chosen from rock formations whose computed mean direction of magnetization had been shown to be significant. The normally polarized rock was taken from a "normal" lava flow and the rock with inverse magnetization from a dyke whose polarization was inverse. To permit accurate measurements, the specimens were selected from a group having reasonably large susceptibilities when measured in weak fields ($k > 4000 \times 10^{-6}$ c.g.s. units). Finally, neither of the specimens used had undergone heat treatment prior to the present investigation.

Both specimens were examined at $H_0 = 2300\,Oe.$, as they cooled from 600°C. To facilitate comparison between them, I_r and I_s were plotted on a scale which made their values at 20°C equal to 1000.

(a) The "normal" basalt, specimen *N*, came from a lava flow in the north eastern part of Mull. The average value of the Curie point obtained from the three curves (Fig. 10) was 572°C, or less than 10°C below that of pure magnetite. The pronounced bend in the H_c–T and I_r–T curves above 250°C suggests the presence of a second constituent, with its Curie point near 300°C.

Koenigsberger [14] examined four German late Tertiary or Quaternary basalts, containing magnetite along with titanium dioxide and excess ferrous oxide and, in one case, pyrrhotite as well. All four specimens had two Curie points each, at temperatures ranging from 450 to 620°C, and 170 to 300°C, respectively. H_c of the basalts at room temperature was between −90 and −175 *Oe.*, compared with −354 *Oe.* obtained after

heat treatment in the present case. However, the coercivity of the high Curie point constituent in *N* was −188 *Oe.* at 350°C, where the H_c–T curve is nearly horizontal; this value appears to be more in agreement Koenigsberger's results. The large coercivity (−534 *Oe.*) before heat treatment may be due to a very small grain size of the ferromagnetic constituents, crystals in volcanic rocks being commonly tiny. The changes in I_r and I_s produced by heat treatment were small, amounting to −10% and +3%, respectively.

(b) The "reversed" specimen, *R*, was a dolerite basalt from a dyke near Dishig, on the south shore of Loch na Keal, Mull. The main features of the three curves (Fig. 11) are simple, but it appears that a major Curie point at about 500°C is followed by that of a minor constituent, at about 600°C. Since I_s and I_r are very small above 500°C, the trend of H_c is doubtful in this region, and it may vanish between 540 and 600°C.

A major second constituent with its Curie point in a lower range of T would have been required, for example, by Néel's two-component mechanisms of reversal. Apart from the small irregularities observed, however, specimen *R* shows the behaviour of a relatively pure ferromagnetic material, whilst specimen *N*, which would be

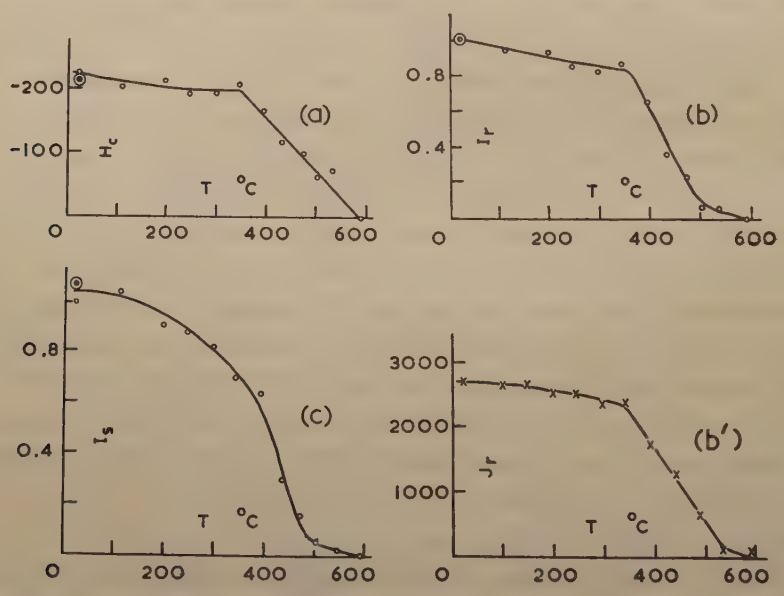

Fig. 11 Specimen *R*. "Reversed" Basalt.
Points obtained ⊙ before heating; ○ whilst cooling; × after cooling.
H_c in oersteds; I_r and I_s in arbitrary units; J_r in c.g.s. units $\times 10^{-6}$.

expected to yield "simple" curves, does reveal a strong second component. The evidence here found thus fails to justify the hypothesis that a property of the material may have caused the original reversal in the polarization of the rock.

Of all the specimens referred to in this paper, *R* showed the least modification of its magnetic properties after heating, the changes in I_r, H_c and I_s being respectively 0, +5 and −7%. It can thus be reasonably claimed that the heat treatment has

caused no important chemical changes and that conclusions drawn from the laboratory data are here applicable to the conditions under which the dyke cooled through its Curie point.

J. Singh [21], until recently of the Geophysics Department, Imperial College, investigated the loss of natural remanent magnetism on heating and examined an inversely magnetized specimen from the same flow as specimen *R*. His results are shown in Fig. 11b', which bears a striking resemblance to the I_r–T curve of specimen *R*. Again, no evidence of a second constituent in significant proportions was found.

It may be suggested that the basalt curves obtained here are, apart from the second constituent of specimen *N*, more truly representative of the properties of magnetite or titanomagnetite than those of the magnetite specimens themselves, $M1$ and $M2$ having changed completely after heating, whilst $M3$ was not examined under saturation conditions.

From the geophysical point of view, the essential feature of both H_c–T curves discussed in this section appears to be the fact that high H_c values were attained in the range 400–500°C. This implies that the basalts were capable of retaining thermoremanence, even at high temperatures, in opposition to an acting field. Together with the failure to find evidence in favour of the two-component mechanism, the data therefore tend to support the hypothesis that a past reversal of the earth's magnetic field has been responsible for the inverse magnetization of the rock formations concerned. However, since they were based on two specimens only, the results must be regarded as supplementary to other evidence.

Summary

Most of the minerals and rocks examined became fully or nearly saturated in an external field of 2300 *Oe*. The specimens behaved like normal ferromagnetic materials, their I_s–T curves broadly resembling those of the ferromagnetic elements. H_c was always large at normal temperatures and, in most cases, it still exceeded -100 *Oe*. at 500°C. It is safe to conclude that the rocks and minerals concerned are capable of retaining thermoremanence for long periods, even at high temperatures.

Irregular features in the temperature curves of some specimens indicated the presence of more than one ferromagnetic constituent. Probably due to chemical action in the material, the hysteresis loops measured at 20°C before and after the heat treatment differed considerably in some instances. In the case of a certain franklinite with its Curie point at about 600°C a new, strongly magnetic, constituent with its Curie point near room temperature appeared after heating.

A comparison of data from two basalts, with respectively normal and inverse directions of natural thermoremanence, gave no indication that a property of the material caused the inverse polarization in one of the rocks. The results supported the hypothesis that such magnetizations owe their direction to past reversals of the geomagnetic field.

Acknowledgments

The author wishes to express his gratitude to Prof. J. M. Bruckshaw for his help and encouragement throughout the work. In addition, the author wishes to thank Dr. G. D. Nicholls of the Geology Department, University of Manchester, for being kind enough to analyze some of the specimens. For their kind assistance whilst at the Geophysics Department, Imperial College, special thanks are due to Dr. J. Singh, Dr. M. Fahim and Dr. S. K. Dutt. The author is also grateful to the Anglo-Iranian Oil Co., and the Anglo-Saxon Oil Co., for providing the financial basis for this research.

References

[1] Bruckshaw, J.M. and Robertson, E.I. Roy. Astron. Soc. Geophys. Suppl. **5**, 308 (1949).
[2] Bruckshaw, J.M. and Vincenz, S.A. Roy. Astron. Soc. Geophys. Suppl. **6**, 579 (1954).
[3] Vincenz, S.A. Roy. Astron. Soc. Geophys. Suppl. **6**, 590 (1954).
[4] Néel, L. Ann. de Phys. **3**, 137 (1948).
[5] Nagata, T. Nature (London) **169**, 704 (1952).
[6] Nagata, T., Akimoto, S., and Uyeda, S. J. Geomag. Geoelec. **4**, 22, 102 (1952). **5**, 168 (1953).
[7] Bruckshaw, J.M. and Rao, B.S. Proc. Phys. Soc. (London) **63**, 931 (1950).
[8] Koenigsberger, J.G. Phys. Zeits. **33**, 468 (1932).
[9] Akimoto, S. Private Communication (1954).
[10] Forrer, R. Jour. Phys. Rad. **2**, 312 (1931).
[11] Akimoto, S. J. Geomag. Geoelec. **6**, 1 (1954).
[12] Akimoto, S. Jap. J. Geophys. **1** (2), 1 (1955).
[13] Roquet, J. Comp. Rend. (Paris) **224**, 1418 (1947).
[14] Koenigsberger, J.G. Terr. Mag. **43**, 119, 299 (1938).
[15] Nagata, T. Rock Magnetism, p. 88 (Tokyo : Maruzen and Co., Ltd., 1953).
[16] Néel, L. Rev. Mod. Phys. **25**, 58 (1953).
[17] Davis, C.W. Physics, **6**, 376 (1935).
[18] Tzu-Chang-Wang. Zeits. f. Geophys. **16**, 160 (1940).
[19] Wologdine, M. Comp. Rend. (Paris) **148**, 776 (1909).
[20] Bates, L.F. Modern Magnetism, p. 323. (Cambridge University Press, 1951).
[21] Singh, J. An Investigation into the process of magnetization of rocks. Ph. D. Thesis, University of London, (1954).

昭和31年12月20日　印刷
昭和31年12月25日　發行
第8卷　第3號

編輯兼發行者　日本地球電氣磁氣學會
代表者　長谷川万吉

印刷者　京都市南区上鳥羽唐戸町63
田中幾治郎

賣捌所　丸善株式會社京都支店
丸善株式會社 東京・大阪・名古屋・仙台・福岡

JOURNAL OF GEOMAGNETISM AND GEOELECTRICITY

Vol. VIII No. 3

1 9 5 6

CONTENTS